Su-AM-N5

EXTRACELLULAR HEMOGLOBIN OF GLOSSOSCOLEX PAULISTUS: EQUILIBRIUM OF DIFFERENT SPECIES IN THE MET FORM.

((Sylvana C.M. Agustinho, Maria H. Tinto, Janice R. Perussi, Marcel Tabak and Hidetake Imasato)), Instituto de Quimica de São Carlos-USP, C.P.780, 13560-970, São Carlos, S.P., Brasil.

Chromatography in Sephadex G-200 of giant whorm extracellular hemoglobin of G.paulistus in the met form evidentiates an unique band at pH 7.0 and two low molecular weight bands at pH 9.0. In the oxidized state (met form) the alkaline dissociation into low molecular weight subunits is complete. The unique band obtained at pH 7.0 corresponds to the whole protein. The two bands at pH 9.0 are assigned to the trimer not completely resolved from the linker chains and the monomer. The molecular weights are very similar to the ones described previously for the oxy form (Biophys. J. 64, A49, 1993). Optical absorption spectra for the whole protein, fraction I, the trimer, fraction II, and the monomer, fraction III, were analyzed as a function of pH. The analysis was carried out using the convex constraint analysis (CCA) programm developed by Fasman et al to study protein secondary structure from C.D. spectra. For the whole protein two pKs of 7.7 and 9.5 were observed corresponding to an irreversible transition from aquomet form to a hemichrome I and an reversible transition from the hemichrome I to hemichrome II. For trimer and monomer fractions only the second reversible transition was observed suggesting the irreversible hemichrome formation. Our results indicate that the hemoglobin of G.paulistus in the met form is quite unstable both regarding the alkaline dissociation and the hemichrome formation. C.D. measurements also suggest a sharp decrease of the Soret band signal upon hemichrome formation implying a weaker heme-globin interaction.

Support : CNP_q, CAPES and FINEP.

Su-AM-N6

DEFINING THE ALLOSTERIC PATHWAY IN HEMOGLOBIN: TIME-RESOLVED UV AND VISIBLE RESONANCE RAMAN SPECTROSCOPY OF KINETIC INTERMEDIATES.

((V. Jayaraman[a], K. R. Rodgers[b], I. Mukerji[c] and T. G. Spiro[a])) [a]Dept. of Chemistry, Princeton University, Princeton, NJ 08544, [b]Department of Chemistry North Dakota State University, Fargo, ND-58105 and [c]Department of Biochemistry and Molecular Biology, Wesleyan University, CT 06457.

Time-resolved resonance Raman spectra were obtained for hemoglobin [Hb] in the nanosecond to microsecond interval following HbCO photolysis. Excitation at 230 nm provides enhancement of tyrosine and tryptophan vibrational modes, which probe different regions of the protein, and complementary experiments with 436 nm excitation provide enhancement of heme vibrational modes, which monitor relaxation of the porphyrin ring and of the Fe-histidine bond, as well as the time course of CO recombination. Spectra of the intermediates are extracted from the transient data. Structural interpretation of these spectra enable the construction of a model for the allosteric transition in Hb, which contains the following features: photolysis of HbCO [A] produces a geminate state [B], in which the CO is trapped in the heme pocket and strain is generated in the heme-F helix linkage. This strain relaxes with a 20 ns time constant, producing intermediate R, in which half the hemes are religated and the E helix is displaced towards the heme in the other half. In turn this displacement relaxes with a time constant of 0.5 μs, producing intermediate S, in which the subunits have rearranged and T-like quaternary contacts have started to form, but the Fe-His bond stays relaxed. Intermediate T is produced with a 17 μs time constant in which the Fe-His bond is strained, as in deoxyHb, and the quaternary contacts are locked in place. However, the H-bond contacts across the $\alpha_1\beta_2$ are weaker than in deoxyHb, and hence it is proposed that the $\alpha_1\beta_2$ interface is deformed as a result of two ligands binding to the same dimer within the tetramer.

Su-AM-N7

STRUCTURAL HETEROGENEITY OF NI(II)-OCTAETHYLPORPHYRIN IN ORGANIC LIQUIDS AND GLASSES.

((M. Leone[1], E. Unger[2], W. Jentzen[3], A. Cupane[1], L. Cordone[1], H. Gilch[2], W. Dreybrodt[2] and R. Schweitzer-Stenner[3])) [1]Insituto di Fisica, University of Palermo, 90123 Palermo, Italy; [2] Institut für Experimentelle Physik, Universität Bremen, 28359 Bremen, Germany; [3] Fuel Science Department, Sandia National Laboratories, Albuquerque, NM 87185, USA.

We have measured the absorption spectrum of Ni(II)-octaethylporphyrin (NiOEP) in CH_2Cl_2 and in a 50% v/v isopentane/ethyl ether mixture as a function of temperature between 150 and 300 K and 40 and 300 K, respectively. The Soret band can be decomposed into two subbands whose frequencies differ by 220 cm^{-1}. By analogy with resonance excitation profiles of conformational sensitive Raman bands (i.e. ν_{10}, ν_{19}) we attribute the low frequency subband to a conformer with a non-planar macrocycle, whereas the high frequency subband is assigned to one or even two planar conformers. The subbands' intensity ratio exhibit a solvent dependent van't Hoff behavior between 300 and 160 K. Crystallization of CH_2Cl_2 prevents measurements at lower temperatures. For NiOEP in the glass forming isopentane/ethyl ether mixture the intensity ratio bends over in a region between 150 K and 100 K and remains constant below. These data can be fitted by a modified van't Hoff expression, which accounts for the freezing into a non equilibrium distribution of the conformers below a distinct temperature T_f. The fit yields a freezing temperature of $T_f \approx 121$ K and a transition region of 52 K. In accordance with Raman data we found that the non-planar conformer has the lowest free energy. Moreover the Soret band's width exhibits a temperature dependent Gaussian contribution. It results from low frequency modes to which the electronic B-state transition is vibronically coupled. This comprises out-of-plane modes of the porphyrin involving the central metal atom, and molecular motions within the liquid environment. At temperatures above the solvent's glass transition the amplitudes of these motions increase above the values predicted by a purely harmonic model. This indicates to non-nharmonic contributions to their potential energy and parallels findings on porphyrins embedded into a protein environment.

Su-AM-N8

POSSIBLE FUNCTIONAL ROLES OF NON-PLANAR CONFORMERS OF TETRAPYRROLES IN PROTEINS.

((J. A. Shelnutt[1,2])) [1]*Fuel Science Department, Sandia National Laboratories, Albuquerque, NM 87185-0710.* [2]*Department of Chemistry, University of New Mexico, Albuquerque, NM 87131.*

Tetrapyrroles in proteins undergo remarkable nonplanar distortions that alter the chemical and photochemical properties of these important cofactors. These non-planar macrocycle conformations are seen in the X-ray crystal structures of many hemoproteins and photosynthetic proteins and are best depicted in the X-ray crystal structures of photosynthetic reaction centers and cytochromes. Recently, it has come to light that a variety of metastable nonplanar conformers may be energetically accessible at physiological temperatures and that these non-equilibrium conformers may be involved in biological function. Both the porphyrin ground-state conformation and these higher energy conformers can influence such properties as reduction potentials, electron-transfer and other reaction rates. Moreover, the protein environment can alter the relative energies of these low energy conformers as a way of regulating the biological properties of the porphyrin cofactor. Antithetically, changes in the metalloporphyrin that occur during its function, such as a change in oxidation state or ligation state of the metal, influence the relative energies of the low energy conformers and their interaction with the protein, allowing the porphyrin to alter the apoprotein moiety. We have devised a quantitative means of classifying these non-planar conformers based on symmetric distortions along only the five lowest-frequency normal mode coordinates of A_{2u} (*doming*), B_{1u} (*ruffling*), B_{2u} (*saddling*), and E_g (*waving*) symmetries of the nominally D_{4h} planar porphyrin. For symmetrically substituted model porphyrins, conformers exhibiting pure distortions with these symmetry properties are often observed. In proteins and non-symmetrically substituted porphyrins, observed distortions are typically composed of linear combinations of distortions alone these five normal coordinates. The possible role of higher energy porphyrin conformers in their biological function will be considered.

(Supported by U.S. DOE Contract DE-AC04-94AL85000.)

SOCIETY AWARD WINNERS SYMPOSIUM

Awards-Sym-1

STRINGS AND MOTORS: BIOPHYSICAL APPROACHES TO SENSORY TRANSDUCTION BY VERTEBRATE HAIR CELLS.

((D.P. Corey)) Mass. Gen. Hospital and Howard Hughes Medical Institute, Boston, MA 02114.

In the current model for transduction and adaptation by hair cells, deflection of the hair bundle towards the tallest stereocilia stretches fine filaments ("tip links") that extend between adjacent stereocilia. These pull on mechanically-sensitive ion channels at the tips of the stereocilia. We tested this model by cutting the tip links (observed by electron microscopy) and found that the mechanical sensitivity is concurrently and irreversibly lost. With Winfried Denk, we used calcium imaging to locate the transduction channels. As in reports, channels are at the tips of stereocilia. They can be at either end, probably both ends, of the tip links. During a maintained deflection, channels adapt towards the resting open probability of about 15%. Howard and Hudspeth speculated that the upper attachment of each tip link can move along the side of the stereocilia, drawn upwards by a myosin-based motor or slipping under excess tension. We measured calcium-dependent rates of adaptation and constructed a mechanical model for adaptation, which successfully predicts a small (~100 nm) voltage-dependent movement of an unrestrained bundle. The incompleteness of adaptation suggests an additional linkage between the motor complex and the actin cores of stereocilia. Cutting the tip links allows the attachment to climb, as observed with TEM. To search for the adaptation myosin, we used degenerate PCR and found ten myosin genes expressed in the sensory epithelium. With Tama Hasson, we found that at least three are expressed in hair cells: myosins VI and VIIa (which cause deafness when defective), and myosin Iβ. As Gillespie and Hudspeth had shown, myosin Iβ is in the tips of stereocilia, making it a candidate for the adaptation motor.

Awards-Sym-3

FRAMESHIFTS, RETROVIRUSES AND PSEUDOKNOTS

(I. Tinoco, Jr., X. Chen, J. V. Hines, H. Kang, L. X. Shen) Department of Chemistry, University of California and Structural Biology Division, Lawrence National Berkeley Laboratory, Berkeley, CA 94720.

Retroviruses synthesize essential viral enzymes—including protease, reverse transcriptase, and integrase—as part of polypeptides produced by minus-one frameshifts as the viral RNA is translated. These programmed frameshifts occur in response to signals composed of a sequence of seven nucleotides at the shift site and a nearby pseudoknot downstream of the shift site. The mechanism of frameshifting is not known, although a pseudoknot might slow or transiently arrest the ribosome at the shift site, and thus promote slippage into the minus-one reading frame. We previously showed that the nucleotide sequence at the junction of the stems of a pseudoknot was important for efficient frameshifting, apparently because it determines a characteristic bent conformation. We have now determined the structures of two pseudoknots with very poor frameshifting ability. One is linear, the other is bent, but in the opposite direction from the efficient frameshifter. The requirement for a precise conformation for efficient frameshifting indicates that a specific interaction occurs between the viral RNA pseudoknot and the host protein-synthesizing machinery.

Su-PM-Sym-1

STRUCTURE AND FUNCTION OF PLANT LIGHT-HARVESTING COMPLEX, LHC-II. ((W. Kühlbrandt and Da Neng Wang))EMBL, Meyerhofstr. 1, D-69117 Heidelberg.

The structure of the light-harvesting chlorophyll *a/b*-protein complex (LHC-II) has been determined by electron microscopy and electron diffraction of two-dimensional crystals. LHC-II, an integral membrane protein, binds roughly half of all pigment molecules involved in plant photosynthesis. The atomic model of the complex shows the structure of three trans-membrane helices, a short amphipathic helix at the membrane surface, and associated chlorophylls and carotenoids. The two central helices are connected through symmetrical ion pairs which also function as chlorophyll ligands. In the centre of the monomer, 7 of the 12 bound chlorophylls, assigned to Chl *a*, are in van-der-Waals contact with two symmetrically placed carotenoids. The arrangement of the pigments in the complex explains the photoprotective function of the carotenoids and helps us to understand the role of the chlorophylls in trapping and transmission of solar energy in the photosynthetic membrane.

Su-PM-Sym-2

STRUCTURE OF THE LH2 ANTENNA COMPLEX FROM PURPLE PHOTOSYNTHETIC BACTERIA. ((R. Cogdell)) University of Glasgow.

Su-PM-Sym-3

FEMTOSECOND DYNAMICS IN BACTERIAL LIGHT-HARVESTING PROTEINS. ((Graham R Fleming, Stephen Bradforth, and Ralph Jiminez)) Dept of Chemistry and James Franck Institute, Univ of Chicago, Chicago IL 60637.

Energy transfer within the symmetric ring structures recently determined for LH 2 and LH 1 has been studied by femtosecond fluorescence polarization and photon echo spectroscopy. We find that in LH 1 coherent vibrational motion apparently suvives several energy transfer hops. Modelling has focused on the nature of the electronic states in these disordered, coupled systems and on simulations of the anisotropy decay. Our current view is that LH 1 is best described as 16 dimers , while in LH 2 delocalization may be a little larger (2-4 molecules). In addition 3 pulse echo and transient grating studies provide the protein spectral density which modulates the electronic energy gaps. This spectral density will form the basis of more sophisticated theoretical models.

Su-PM-Sym-4

MODELING EXCITATION TRANSFER DYNAMICS IN ANTENNA COMPLEXES OF KNOWN STRUCTURE. ((K. Sauer)) Chemistry Dept. and Structural Biology Division, LBNL, Univ. of California, Berkeley, CA 94720.

Photosynthetic antenna pigment proteins function by absorbing light, transferring electronic excitation rapidly among the chromophores within the protein and then from one antenna complex to another toward the reaction center. The mechanism of this transfer can be learned through spectroscopic studies of antenna complexes whose detailed molecular structure has been determined by crystallographic methods. Successful modeling results in accurate predictions of excited-state dynamics, as probed spectroscopically by bleaching/recovery, fluorescence decay and anisotropy relaxation. Where stronger exciton interactions occur among the pigments, characteristic features appear in the absorption, CD and linear dichroism spectra. Excited-state relaxation in phycocyanin from cyanobacteria can be understood largely in terms of the Förster inductive resonance theory. By contrast, in the LH2 protein from purple photosynthetic bacteria, the bacteriochlorophylls are closely coupled to one another, resulting in delocalized excited states and pronounced spectroscopic splittings. These examples illustrate the two limiting cases that occur in photosynthetic antenna proteins.

SODIUM CHANNELS I

Su-PM-A1

A SPECIFIC ENERGETIC COUPLING SUGGESTS THE ORIENTATION OF μ-CONOTOXIN GIIIA WITH RESPECT TO THE Na^+ CHANNEL OUTER VESTIBULE. ((S.C. Dudley, J.L. Penzotti, G. Lipkind, R.J. French, H.A. Fozzard)) University of Chicago, Chicago, IL 60637.

Based upon protein folding predictions and the effects of site-directed mutagenesis of the channel on saxitoxin and tetrodotoxin blocking, we recently proposed a molecular model of the outer vestibule of the voltage-gated Na^+ channel. Using this model, we have made predictions about interactions of the outer vestibule with μ-conotoxin GIIIA (μ-CTX), a positively charged toxin of known structure which binds channels from adult rat skeletal muscle (μI) and eel electric organs. Mutagenesis of μ-CTX has suggested that the guanidinium group of R13 is required for complete block of single channel currents (Becker et al., *Biochemistry 31*, 8229, 1992.). Based on this idea that R13 occludes the pore, the most energetically favorable orientation of μ-CTX with respect to the model of the outer vestibule was calculated (Dudley et al., *Biophys. J.* 1995. In press.). In this orientation, Q14 of μ-CTX was in proximity to E758 of μI. This hypothesis was supported further by mutant cycle analysis. Neutralization of E758 (E758Q) was undertaken by PCR. Introduction of a negative charge at Q14 of μ-CTX was carried out by solid phase synthesis. The effect of mutations of the toxin or the channel were determined by measuring the equilibrium 50% inhibitory concentration of toxin (IC_{50}) applied to *Xenopus* oocytes. Peak currents before and after exposure to the toxin were measure using two microelectrode voltage clamp. The four possible combinations of toxin and channel Q14•E758, Q14D•E758, Q14•E758Q, and Q14D•E758Q showed IC_{50}s of 17 ± 5 (n=8), 404 ± 47 (n=11), 822 ± 105 (n=11), and 713 ± 37 (n=4), respectively (mean ± SEM in nM). The ability of the mutation E758Q to eliminate the decrease in binding associated with the mutation Q14D was consistent with the model prediction of a close approximation of Q14 and E758 and with a calculated coupling coefficient (Hildago and MacKinnon *Science 268*, 307, 1995), Ω, of 27. Further, a close interaction explains the observation that Q14D•E758Q has improved binding compared with Q14•E758Q. The interactions of R13 with the selectivity filter and of Q14 with E758 serve to orient the toxin with respect to the outer vestibule.

Su-PM-A2

STUDY OF μ-CONOTOXIN SENSITIVITY ON CHIMERIC HUMAN HEART /SKELETAL MUSCLE SODIUM CHANNELS EXPRESSED IN *XENOPUS* OOCYTES.((M. Chahine, L.-Q. Chen and R. G. Kallen)) Laval Hospital, Research Center, 2725, Chemin St.-Foy, St.-Foy, Québec, Canada G1V 4G5 and Department of Biochemistry and Biophysics, University of Pennsylvania School of Medicine, Philadelphia, PA 19104-6059.

It is known that in native tissue heart sodium channels are 10^3 fold more resistant to block by tetrodotoxin and μ-conotoxin than are skeletal muscle sodium channels. In this study we take advantage of human heart (hH1, μ-conotoxin insensitive, IC_{50}>3μM)) and skeletal muscle (rSkM1, μ-conotoxin sensitive, IC_{50}=51.4nM), two cloned sodium channels to identify the nature of this important pharmacological difference. Chimeras in which one or several domains (D) where interchanged between rSkM1 and hH1 were constructed and μ-conotoxin was tested on sodium currents expressed in *Xenopus* oocytes using two microelectrode voltage clamp. When D1 and D2 are from rSkM1 and D3 and D4 are from hH1, the affinity of μ-conotoxin to this chimera was found to be higher (11.9 ± 1.5nM) compare to wild-type rSkM1. This four fold increase in the affinity is likely to result from the three fold increase in k_{on}. The chimera in which D1 is from hH1 and D2,3 and 4 are from rSkM1 was barely sensitive to μ-conotoxin (IC_{50}=1.4 ± 0.2 μM). However chimera in which D1,2 and 3 are from rSkM1 and D4 is from hH1 was sensitive to μ-conotoxin (IC_{50}=36 ± 3nM). We tested also whether D 3 plays any role in this toxin sensitivity by constructing chimera in which D1,2 and 4 are from rSkM1 and D3 was from hH1. The expressed currents were as sensitive to μ-conotoxin as is rSkM1, suggesting that D3 plays no role in the difference between rSkM1 and hH1 in their sensitivity to μ-conotoxin. However these data indicate that the main difference between hH1 and rSkM1 in terms of their sensitivity to μ-conotoxin appears to be located in D1. (Supported by grants from MRC to MC and NIH to RGK).

Su-PM-A3

DEPTH ASYMMETRIES OF THE FOUR SODIUM CHANNEL P SEGMENTS REVEALED BY DIFFERENCES IN CADMIUM BLOCK AND SIDE CHAIN ACCESSIBILITY OF CYSTEINE MUTANTS. ((M. Teresa Pérez-García, Nipavan Chiamvimonvat, Ravi Ranjan, Eduardo Marban, Gordon F. Tomaselli)) Johns Hopkins University, Baltimore, MD 21205.

We have used serial cysteine mutagenesis in the P segments of the voltage-gated μ1 Na^+ channel to study the structure of the outer vestibule and selectivity region. Single-channel analysis of the voltage-dependence of Cd^{2+} block enabled us to determine the location within the electrical field of cysteine-substituted mutants in the P segments of all four domains. The fractional electrical distances of the substituted cysteines was compared with the differential sensitivities to modification by hydrophilic, sulfhydryl-specific modifying reagents of varying size and charge. The P segments of the four domains are not in register. Sequence-aligned residues in domains I and III bind Cd^{2+} with similar voltage dependence, suggesting a similar depth within the electrical field. In contrast, sequence-aligned residues in domains II and IV bind with shallower and steeper voltage dependences, respectively. Thus, the P segment of domain II is relatively external, while the domain IV P segment is deeper as compared to the first and third domain P segments. Sulfhydryls that exhibited the steepest voltage-dependence for Cd^{2+} block are the only ones that are differentially modified by methanethiosulfonate reagents of differing size and charge. For example, K1327C and A1529C are accessible only to the smallest of these compounds, the cationic MTSEA. Our data demonstrate that, unlike K^+ channels, the P segments of the Na^+ channel are not symmetrically disposed along the axis perpendicular to the membrane.

Su-PM-A4

CONTROL OF ION FLUX AND SELECTIVITY BY NEGATIVELY CHARGED RESIDUES IN THE OUTER MOUTH OF RAT SODIUM CHANNELS. ((N. Chiamvimonvat, M. T. Pérez-García, G. F. Tomaselli and E. Marban)) Johns Hopkins University, MD 21205.

The sodium channel has a ring of negatively charged amino acids on its external face. This common structural feature of cation-selective channels has been proposed to optimize conduction by electrostatic attraction of permeant cations into the channel mouth. We tested this idea by mutagenesis and chemical modification of μ1 rat skeletal sodium channels expressed in *Xenopus* oocytes. Replacement of the external glutamate residue in domain II by cysteine (E758C) reduces sodium current by decreasing single-channel conductance. While this effect can be reversed by the negatively charged sulfhydryl-specific modifying reagent MTSES, the flux saturation behavior cannot be rationalized simply by changes in the surface charge. The analogous mutations in domains I, III and IV, E403C, D1241C and D1532C, affect not only conductance but also selectivity. Unlike wild-type channels, the D1532C mutant exhibits appreciable permeability to K^+ and NH_4^+ ions. Our findings necessitate revision of prevailing concepts regarding the role of superficial negatively charged residues in the process of ion permeation. These residues do not act solely by electrostatic attraction of permeant ions, but instead may help to form ion-specific binding sites within the pore.

Su-PM-A5

MOLECULAR DIMENSIONS OF THE SODIUM CHANNEL PORE REVEALED BY DOUBLE CYSTEINE MUTAGENESIS.((J-P. Bénitah, E. Marban, G. F. Tomaselli)). The Johns Hopkins University, Baltimore, MD. (Spon. by H. Kusuoka).

Double mutants can provide unique insights into protein structure by thermodynamic mutant cycle analysis and, in the case of double cysteine mutagenesis, by the ability of neighboring residues to form disulfide bonds. We used both of these approaches to probe the relative proximities of various residues within the rat skeletal muscle Na^+ channel. Cadmium and zinc block affinities served as sensitive assays for the interaction of any given cysteine mutant with pore-blocking particles of known dimension. Combining mutations which individually increase sensitivity to block by Cd^{2+} or Zn^{2+} may have any of three possible consequences: positive cooperativity for binding the divalent cation, suggesting the formation of coordination site; negative cooperativity suggesting the formation of a disulfide bond between the substituted cysteines (in which case their α carbons must be within 7 Å of each other); or no cooperativity consistent with two independent binding sites. We paired the domain I mutant Y401C with a variety of other cysteine mutants in domains II, III and IV. While most of the double mutants have independent, non-interacting cation binding sites, interaction energy and mutant cycle analysis revealed a key residue which created a coordination site that bound Cd^{2+} cooperatively when paired with Y401C (excess of $\Delta\Delta G_i$=2 kcal/mole). In the same double mutant, Zn^{2+} exhibited no cooperativity. Another double mutant was remarkable in its unambiguous ability to form a disulfide bond that partially occluded the pore; a cooperative Cd^{2+}- and Zn^{2+}-binding site could be created by exposure of this mutant to the reducing agents glutathione or DTT. Double-cysteine mutagenesis has the remarkable potential to define regions of close proximity by distinctive alterations of the function of an intact protein.

Su-PM-A6

ALTERED IONIC SELECTIVITY OF THE Na^+ CHANNEL REVEALED BY CYSTEINE MUTATIONS IN THE P-LOOP OF DOMAIN IV
((Robert Tsushima, Ronald Li, and Peter Backx)) Depts. of Medicine and Physiology, University of Toronto, Toronto, Canada.

Introduction of cysteine residues into the pore region of the rat skeletal Na^+ channel (μ1-2) has allowed us to study the interaction of Cd^{2+} and the membrane-impermeant methanethiosulfonate compounds with the mutated channel. This provides us with information on the spatial orientation of the pore residues. We further studied the contribution of the pore residues to ionic selectivity. The μ1-2 and cysteine mutated channels were coexpressed with the rat brain ß1 subunit in *Xenopus* oocytes. Ionic selectivity of the channels was examined by replacing Na in the bathing solution with other monovalent cations (Cs, K, Li, NH_4). The μ1-2 channel displayed an ionic selectivity $Na > Li > NH_4 > K > Cs$. Mutations within the P-loop of domain IV dramatically altered the sequence of selectivity, such that the selectivity of W1531C was $NH_4 > K > Na > Li > Cs$ and D1532C was $Na > Li = NH_4 > K > Cs$. Other mutations within domain IV (T1527C, S1528C, A1529C, G1530C) displayed a similar selectivity as μ1-2. Sulfhydryl modification of W1531C or D1532C with either the positively or negatively charged methanethiosulfonate compounds (MTSEA and MTSES, respectively), did not alter the sequence of the ionic selectivity of these mutants. Cysteine mutations within the P-loops of domains I, II and III exhibited a less dramatic alteration in ionic selectivity such that the sequence was $Li \geq Na > NH4 > K > Cs$. These data suggest that the tryptophan and aspartate residues in domain IV play a critical role in determining the ionic selectivity of the rat skeletal Na^+ channel.

Su-PM-A7

DETERMINATION OF NA^+ CHANNEL PORE STRUCTURE USING SINGLE AND MULTIPLE CYSTEINE SUBSTITUTIONS
((Ronald Li, Robert Tsushima and Peter Backx)) Depts. of Medicine and Physiology, University of Toronto, Toronto, Canada.

Cysteine substitution of a tyrosine residue (i.e. Y401C) in the pore of skeletal muscle Na^+ channels (SkM) creates a 200-fold increase in sensitivity to the group IIB divalents (i.e. Cd^{2+}, Zn^{2+}) (Backx et al, *Science 257:248-251, 1992*). Therefore, we postulated that cysteine substitution of amino acids located in the P-loops of repeats I-IV of Na^+ channels would allow identification of amino acids lining the pore by examining changes in sensitivity to Cd^{2+} block. All cysteine mutants in the SS2 domain of the P-loops, except I757C and W758C, show marked increases in sensitivity to Cd^{2+} block. Replacement of two residues in separate repeat domains created a number of mutant channels exhibiting sensitivities to Cd^{2+} which were 5-20 fold greater than either of the single mutants. Since Cd^{2+} (like Zn^{2+}) is capable of coordinately binding to multiple sulfhydryl residues, our results suggest that, in double mutants with elevated Cd^{2+} sensitivity, the residues are able to coordinately bind Cd^{2+} ions. Using these results and the strict geometric constraints associated with coordinated Cd^{2+} binding, a detailed three-dimensional structure model of the Na^+ channel pore can be constructed in which the proximity of residues to one another is experimentally determined.

Su-PM-A8

MOLECULAR DETERMINANTS OF VOLTAGE-GATED SODIUM CHANNEL $\alpha-\beta_1$ SUBUNIT INTERACTION ((N. Makita, P. B. Bennett, A. L. George.)) Vanderbilt University, Nashville, TN 37232

The β_1 subunit is an integral component of heteromultimeric voltage-gated Na^+ channels. In the *Xenopus* oocyte expression system, β_1 modulates the gating behavior of recombinant brain and skeletal muscle Na^+ channel $\alpha-$subunits but has little or no effect on a cloned human cardiac Na^+ channel (hH1). Expression of a recombinant human skeletal muscle Na^+ channel α subunit (hSkM1) in oocytes gives rises to currents that exhibit slow macroscopic inactivation in the absence of β_1 (τ_h=10.8±0.7 msec), and β_1 co-expression confers a rapid inactivation phenotype (τ_h=1.5±0.1 msec). In contrast, hH1 exhibits fast inactivation (τ_h=2.1±0.1 msec) in oocytes and its gating kinetics are changed little, if at all, by β_1 co-expression (τ_h=2.5±0.1 msec). To localize structural determinants of the β_1 response, we have studied chimeric hSkM1/hH1 channels expressed in *Xenopus* oocytes by two-electrode voltage-clamp recording. Time constants for macroscopic inactivation (τ_h) were derived from single exponential fits of current tracings obtained with a test pulse of −20mV from a holding potential of −120mV. Using this approach, we have identified two α subunit structures that are required for β_1 response. The modulatory effect of β_1 on inactivation was absent in a chimera formed by transplanting the S5-S6 interhelical loops from domain I (D1) and D4 from hH1 to hSkM1. An attenuated β_1 response was observed when only one of these loops were transplanted, but a normal response was seen in chimeras formed with D2 and D3 loops. In contrast, a chimera (hH1-P14) in which the D1/S5-S6 and D4/S5-S6 loops from hSkM1 were transplanted into hH1 exhibited rapid inactivation (τ_h=2.6 ±0.2 msec) similar to wild-type hH1, and co-expression of β_1 significantly accelerated inactivation (τ_h=1.3±0.1 msec) indicating that the transplanted segments conferred β_1 responsiveness. These results suggest that β_1 interacts with S5-S6 loops in D1 and D4 which are brought in close proximity by the tertiary folding of the channel.

Su-PM-B1

TROPONIN- I AND TROPONIN- T INTERACT WITH TROPONIN- C TO PRODUCE DIFFERENT Ca^{2+}-DEPENDENT EFFECTS IN THE MOTILITY ASSAY.

((S.B.Marston and I.D.C. Fraser))
NHLI (CM), Imperial College, Dovehouse Street, London SW3 6LY, UK.

We have analysed how troponin-tropomyosin controls movement of phalloidin-rhodamine labelled actin filaments over skeletal muscle HMM immobilised on a siliconised glass surface. Conditions were obtained where at least 80% of actin-tropomyosin filaments were motile. The effect of adding troponin at pCa 9 was to decrease the proportion of filaments motile to less than 20% with no dissociation of the filaments from the HMM surface or change in velocity of the filaments that moved. The whole filament switched as a unit independent of its length (<2 to>15 μM). Parallel visualisation of troponin on the filaments with anti TnT Mab (tagged with fluoresceine-anti mouse IgG) showed that the switch was not due to co-operative Tn binding to the filaments. This suggests that it is the probability of the filament being in either the on or the off state which is controlled by Tn. Software has been devised for automatic analysis. Up to 100 filaments are located in a pair of images taken at an interval of 0.5-1 sec and 10 or more such pairs are analysed for each assay (around 700 individual measurements). The proportion of filaments motile, velocity of motile filaments and density of filaments on the HMM surface are then calculated. Titration of actin-Tm-Tn with Ca2+ (pCa 9-pCa 4.5) revealed a dual regulatory effect: Ca2+ switched filaments from 15% motile to 90% motile but also increased filament velocity from 3.3 to 5.2 μm/sec. We have demonstrated that the two effects are due to separate interactions of TnC with TnI and TnT. When the complex actin-Tm-TnI+TnC was titrated with Ca2+, motility was switched on but velocity of motile filaments did not change. When the complex actin-Tm-TnT+TnI+TnC was titrated, both the proportion of filaments motile and velocity were increased by Ca2+. This assay therefore permits the analysis of the individual contributions of TnT and TnI to regulation in the troponin complex.

Su-PM-B2

FUNCTIONAL SIGNIFICANCE OF ASP 89 OF THE TROPONIN C CENTRAL HELIX

((S. Ramakrishnan and S. E. Hitchcock-DeGregori)) Department of Neuroscience and Cell Biology, UMDNJ-Robert Wood Johnson Medical School, Piscataway, NJ 08854.

The central helix of troponin C is highly conserved in length and amino acid sequence. Previous work from our laboratory and others has shown the importance of the TnC central helix for thin filament regulation. In this region, Asp 89 is highly conserved and specific to TnC. To investigate the significance of this residue we constructed three mutants: 1. Asp 89 of wild type was replaced with Ala (D89A); 2. the central helix was replaced with a custom designed α-helix (αhrep) consisting of ^{87}AEAALKAAMEA^{97}; and 3. Ala 89 of αhrep was replaced with Asp (A89D). All mutants were tested *in vitro* for the regulation of actomyosin ATPase activity in a fully reconstituted thin filament system. D89A and αhrep were defective in the activation of the actomyosin ATPase activity in the presence of Ca^{2+} and both had only 30% of the wild type maximal activity. A89D was normal in activating the actomyosin ATPase activity in the presence of Ca^{2+}, but defective in inhibition without Ca^{2+}. Interestingly, A89D, unlike wild type, was able to form a complex with TnT even in the absence of Ca^{2+} in non-denaturing polyacrylamide gels. In addition, in A89D the Ca^{2+} concentration required for half-maximal activation (K_d) of actomyosin ATPase was lower (1.5 x 10^{-7} M) compared to wild type (3 x 10^{-7} M). The Ca^{2+} dependence of D89A and αhrep was shifted to a significantly higher concentration and was less cooperative. The Ca^{2+} affinity (monitored by CD) for both low and high sites was higher in A89D than in wild type while there were no changes in D89A. However, the Ca^{2+} affinity was severely affected in αhrep. Our results strongly suggest that Asp 89 is crucial for TnC function and possibly for its interaction with other troponin components. (Supported by NIH and AHA, NJ).

Su-PM-B3

FLUORESCENCE RESONANCE ENERGY TRANSFER MEASUREMENTS OF ACTIVATED MYOSIN LIGHT CHAIN KINASE.

((B.A. Clack, C. Cremo*, G. Zhi, J.K. Krueger, J.T. Stull)) Physiology Dept., UT-Southwestern Medical Center, Dallas, TX 75235-9040; * Dept. Of Biochemistry and Biophysics, Washington State Univ., Pullman, WA, 99164-4660;

It has been proposed that myosin light chain kinase activity is regulated by an intrasteric mechanism whereby the linker region between the calmodulin binding sequence and the catalytic core physically move upon binding Ca^{2+}/calmodulin (CaM), exposing the regulatory light chain (RLC) binding site. Fluorescence Resonance Energy Transfer (FRET) was measured between extrinsic probes on CaM, RLC, and an ATP analog, TNP-AMPPNP, when each of these ligands was bound to the rabbit skeletal muscle myosin light chain kinase (MLCK) (residues 256-607). The thiol-specific fluorophore IAEDANS (donor probe) was incorporated into recombinant CaM at residues 3 and 146 respectively and at position P+4 (residue 23) relative to the phosphorylatable Ser19 in recombinant RLC after mutating the respective residues to Cys. TNP-AMPPNP was the acceptor probe for distances measured to the ATP binding site. When distances between CaM and the RLC were determined, IAF was the acceptor probe in RLC at residue 23. The measured distances between the N-terminus and the C-terminus of CaM to TNP-AMPPNP was 25Å and 19Å, respectively. The respective distances between P+4 in RLC and TNP-AMPPNP or the N-terminus of CaM were 20 Å and 34Å, respectively. These results suggest that CaM bound to MLCK remains in close proximity to the catalytic site and the bound RLC.

Su-PM-B4

THIN FILAMENT ACTIVATION IS NOT PROPORTIONAL TO TNC REGULATORY SITE CA^{2+} BINDING. STUDIES OF CARDIAC THIN FILAMENTS CONTAINING MIXTURES OF TNC AND REGULATORY SITE MUTANT TNC

((Tobacman, LS and Butters, CA)) Depts. of Int. Med. and Biochemistry, Univ. of Iowa, Iowa City, IA 52242

Cardiac thin filaments were assembled containing 14 μM actin, 2.5 μM tropomyosin, and 2 μM of a mixture of troponin and/or troponin inactivated by mutagenesis (D65A) of cardiac TnC site II, the sole regulatory Ca^{2+} binding site. In the presence of 0.1 mM $CaCl_2$, these thin filaments have a fractional saturation of the regulatory sites that is experimentally dictated by the ratio of added troponin to the sum of troponin plus mutant troponin. The myosin S-1 MgATPase rate produced by these thin filaments was linear with myosin S-1 concentration over a 16-fold range, but was not linear with respect to fractional Ca^{2+} binding to the regulatory sites. ATPase activation lagged behind Ca^{2+} binding, with only 30% activation in the presence of 50% Ca^{2+} saturation. In separate experiments, the Ca^{2+} concentration dependence of ATPase activation was shown to be the same for thin filaments with either 100% or 25% normal TnC (and 0% or 75% mutant TnC). This suggests little effect of one troponin on Ca^{2+} binding to an adjacent troponin. This conclusion is also supported by a statistical mechanical analysis of competitive binding of the two forms of troponin to the thin filament. The paradoxical implication is that Ca^{2+} binding very cooperatively increases the ATPase rate despite very little cooperativity in Ca^{2+} or myosin S-1 binding to the thin filament. To rationalize the data we suggest: (1) the cross-bridge cycle involves a conformational change in the thin filament; (2) this conformational change requires Ca^{2+} binding to the TnC nearest to the bound myosin, and also to an adjacent TnC.

Su-PM-B5

UNCOUPLING THE Ca^{2+}-INDUCED CONFORMATIONAL TRANSITION IN THE C-TERMINAL DOMAIN OF CALMODULIN.

((D.F. Meyer & Z. Grabarek)) Muscle Research Group, Boston Biomedical Research Institute, 20 Staniford St., Boston, MA. 02114.

There are two structurally similar classes of EF-hand-type Ca^{2+}-binding proteins: the regulatory proteins (e.g., Calmodulin (CaM)) which undergo a Ca^{2+}-induced conformational transition and the Ca^{2+}-buffering proteins (e.g., Calbindin D_{9K}) which do not exhibit such a transition. In a search for the structural elements that distinguish these proteins we have introduced mutations into the Ca^{2+}-binding loop III of the C-terminal fragment of CaM (C-CaMW; residues 77-148) to resemble loop I of calbindin D_{9K}. Specifically (1) The invariant Asp at position one in the loop is replaced by two Ala residues and Asn inserted between position 6 and 7 (C-CaMBL3). (2) Mutation #1 plus Asn at position 5 and the invariant Gly at position 6 replaced by Asp and Pro respectively (C-CaMBL5). The Ca^{2+}-titration curves indicate that cooperativity between the two Ca^{2+}-chelating loops has been lost in both mutants. There is a decrease in Tyr fluorescence of C-CaMBL3 over a broad range of [Ca^{2+}]. C-CaMBL5 exhibits an increase in Tyr fluorescence at low [Ca^{2+}] followed by a decrease in fluorescence at high [Ca^{2+}]. The latter most likely corresponds to Ca^{2+}-binding at the mutated site III. Far UV CD shows a larger Ca^{2+}-dependent increase in α-helical content in both mutants as compared to C-CaMW and a lower structural stability as indicated by a 15°C decrease in melting temperature. Binding of bisANS and of a synthetic peptide (an analogue of the CaM binding site of myosin light chain kinase) to both mutants are reduced compared to C-CaMW. These results indicate that conversion of loop III in C-CaM to a 14 residue pseudo EF-hand loop characteristic of calbindin D_{9K} caused a loss of cooperativity between the Ca^{2+} binding sites and an impairment of the conformational transition. (Supported by NIH, AR-41156)

Su-PM-B6

EVALUATION OF THE POSITION OF TAXOL® MOLECULE AT ITS BINDING SITE ON THE MICROTUBULES

((R.Nicholov, W.Ho and F.DiCosmo)) IBME, University of Toronto, Ontario, Canada M5S 3B2

Taxol® is a diterpenoid used as an antimitotic drug. Taxol® action is antagonistic to the other tubulin directed drugs; it blocks depolymerization of tubulin. The spin labelled taxol® analogues were synthesized. TEMPO or TEPYRO were attached at three different positions of Taxol® with the goal of enhancing anticancer efficacy and creating new instruments for studying the conformation of tubulin molecules during the process of polymerization, attachment site of taxol® and its orientation towards the tubulin.

The comparison between ESR spectra of spin labelled Taxol® SP-C7 in buffer and SP-C7 in reaction medium (with tubulin and GTP) at 273°K (no polymerization), shows that the attachment of SP-C7 to ß-tubulin does not change significantly the ESR parameters. However if the polymerization is induced the differences between the ESR spectra in the buffer and in reaction medium at corresponding temperatures increase. Already at 288° K the splitting of the low magnetic field resonance line occurs. A dramatic alteration of the ESR spectrum occurs at 310 and continues at 313 K. These data show that nitroxyl radical attached to C7 carbon atom of taxol® molecule is strongly affected by the polymerization process. ESR spectra show that polymerization immensely restricts the rotational mobility of this spin probe. The same experiments performed with SP-C2 and SP-C3' Taxol show a different immobilization pattern. These results help evaluate the position and orientation of taxol® toward microtubules.

Su-PM-B7

THE ROLE OF TITIN IN MUSCLE SARCOMERE FORMATION, A GENE-TARGETING APPROACH. ((D.M. Wright & M. Peckham.)) The Randall Institute, King's College London, 26-29 Drury Lane, London, WC2B 5RL. UK

Titin is a large (~3500kD) myosin binding protein found in striated muscle, that spans from the Z disc (N terminus) to the M line (C terminus). From sequence analysis and antibody studies it has been suggested that titin may regulate the length of the myosin thick filament, and organize it into the muscle sarcomere. To test these ideas, we plan to knock out the expression of titin in novel conditionally immortal myogenic cells (Morgan *et al.*, 1994, Dev. Biol. **162**, 486-498) and determine the effects of loss of titin on thick filament and sarcomere assembly. We chose to do this in myogenic cells in culture as a knockout of titin in transgenic mice is likely to be lethal. We have recovered an isogenic genomic DNA clone that includes coding sequence for the region of titin just outside the Z-disc. We manipulated this clone *in vitro* to interrupt the coding sequence with a mutant pMC1neo gene, to truncate transcription and translation of the gene and allow for positive selection by resistance to G418. We cloned the TK gene outside the region of genomic DNA to allow for negative selection (Mansour *et al.*, 1988 Nature, **336**, 348-352). Cells that have undergone homologous recombination with the targeting DNA do not incorporate the TK gene and are resistant to gancyclovir (GANC). These targeting constructs have been electroporated into the myogenic cells and we have screened roughly 100 $G418^r$, $GANC^r$ clones by PCR for targeted events. PCR positive clones are now being analysed by southern analysis to confirm whether the first allele has been targeted. By using the mutant neo gene in the targeting construct and selecting with a low G418 concentration initially, we should then be able to knockout the second allele simply by increasing the G418 concentration for targeted cells, which encourages intrallelic recombination. We plan to investigate the effects of the titin mutation on sarcomere formation in singly and doubly targeted cells, when the cells differentiate into myotubes. We thank Matthias Gautel and Siegfried Labeit for cDNA probes. Supported by Human Frontiers, Royal Society and BBSRC.

FOLDING AND SELF-ASSEMBLY: STABILITY AND INTERMEDIATE STATES A26

Su-PM-C1

HEMOGLOBIN STRUCTURE PROBED BY FLUORESCENCE SPECTROSCOPY UNDER HIGH HYDROSTATIC PRESSURE. ((Z. Gryczynski, J. Lubkowski, S. Beretta and E. Bucci.)) Dept. of Biochemistry, University of Maryland Medical School at Baltimore, Maryland.

The effect of hydrostatic pressure on the native human adult hemoglobin were investigated by monitoring changes of steady-state and time-resolved intrinsic tryptophan fluorescence. Hydrostatic pressure promoted significant increase of fluorescence intensity together with a small red shift of maximum of the emission spectrum. Time-resolved analyses showed multiexponential decay of tryptophan excited state with three lifetime components. As shown by the Table below pressure strongly affected the amplitudes of the two longer lifetime components (below 1 ns and around 4 ns) together with an increased length of the intermediate component (from 313 ps to 730 ps). The Förster model of radiationless excitation energy transfer between tryptophan and heme allowed interpretation of the observed lifetime distribution in terms of protein dissociation into dimers and monomers. The data also showed that subunits dissociation was strongly correlated with reversible release of heme from the heme pocket of the monomers. The reversible heme dissociability observed at hydrostatic pressure above 1 kbar suggests a volume change produced by the collapse of the heme pocket. Lower reversibility of this phenomenon after long exposure to high hydrostatic pressure above 2 kbar suggests that monomer formation and destabilization of the heme pocket initiate protein unfolding.

Pressure (kbar)	τ_1[ps]	α_1	τ_2[ps]	α_2	τ_3[ps]	α_3
0.001	21	0.987	313	0.010	3650	0.003
1000	24	0.955	672	0.038	4182	0.007
1700	33	0.892	730	0.078	3105	0.030

Su-PM-C2

COMPRESSIBILITY AS A UNIQUE MEANS TO DETECT AND CHARACTERIZE GLOBULAR PROTEIN STATES ((Tigran V. Chalikian and Kenneth J. Breslauer)) Department of Chemistry, Rutgers, The State University of New Jersey, Piscataway, NJ 08855-0939

We report compressibility data on single domain, globular proteins which suggest a general relationship between protein conformational transitions and $\Delta k°_S$, the change in the partial specific adiabatic compressibility which accompanies the transition. Specifically, we find transitions between native and compact intermediate states to be accompanied by small increases in $k°_S$ of +(1 to 4) × 10^{-6} $cm^3g^{-1}bar^{-1}$. By contrast, transitions between native and partially unfolded states are accompanied by small decreases in $k°_S$ of -(3 to 7) × 10^{-6} $cm^3g^{-1}bar^{-1}$, while native-to-fully unfolded transitions result in large decreases in $k°_S$ of -(18 to 20) × 10^{-6} $cm^3g^{-1}bar^{-1}$. Thus, for the single domain, globular proteins studied here, changes in $k°_S$ correlate with the type of transition being monitored, independent of the specific protein. Consequently, $k°_S$ measurements may provide a convenient approach for detecting the existence of and for defining the nature of protein transitions, while also characterizing the hydration properties of individual protein states.

Su-PM-C3

Thermal unfolding of human high-density apolipoproteins A-I and A-II.
Olga Gursky and David Atkinson, *Department of Biophysics, Boston University School of Medicine, Boston MA 02118-2314*

Apolipoproteins A-I (M_w 28 kD) and A-II (disulfide-linked dimer of M_w 17 kD) are the major proteins of high-density lipoproteins (HDL) and are critically involved in the transport and metabolism of cholesterol. To understand the relation between the structure, energetics, and functions of A-I and A-II on HDL, we analyzed the thermal unfolding of apoA-I and apoA-II under near-physiological solvent conditions in the temperature range from -8° to +90° using far- and near-UV CD and differential scanning calorimetry. ApoA-I undergoes an extended non-two-state heat denaturation from 25° - 90° with midpoint T_d=57°, suggesting nearly independent unfolding of 6-7 long α-helixes constituting ~60% of its secondary structure. Thermodynamic analysis of apoA-I unfolding suggests that lipid binding and exchange of apoA-I between HDL may be mediated via the molten-globular apolipoprotein state in plasma. In contrast to apoA-I, apoA-II unfolds with apparent two-state kinetics both upon heating and cooling from 25°, indicating the presence of a substantial hydrophobic core in the folded state. Reversible disruption of apoA-II secondary structure by cooling (T_d=-5°) is more extensive and cooperative compared to the heat denaturation (T_d= 53°). Analysis of the effects of buffer composition, pH and protein concentration on the kinetics of apoA-II refolding from the cold-denatured state provide new insights into the possible physiological action of apoA-II.

Su-PM-C4

PREMOLTEN GLOBULE STATE OF α-LACTALBUMIN DETECTED BY CIRCULAR POLARIZATION OF FLUORESCENCE. ((E.E.Gussakovsky, E.Haas)) Department of Life Sciences, Bar Ilan University, Ramat Gan 52900, Israel

Circular polarization of tryptophan and ANS fluorescence (trp-CPF and ANS-CPF) was applied in order to determine experimentally the existence of an intermediate in the transition of Ca^{2+}-saturated bovine-α-lactalbumin (α-LA) from native (N) to acid (A) state which is known as a molten globule. The CPF method was shown to be effective in protein studies (Steinberg, Gafni et al., 1972-1995). The pH dependence of both near-UV CD and ANS-fluorescence intensity of α-LA solutions showed a single transition at pH 3-3.7 as already reported elsewhere and indicated the transition from N- to A-state. The pH dependence of both trp-CPF and ANS-CPF showed an additional conformational transition at pH 4-5 which coincided with the pK of Ca^{2+}-dissociation (pK~5). There is a pH range of 3.7-4.1 in which α-LA exist in an intermediate state between N- and A-states. This intermediate resembles the "critical activated state" deduced theoretically (Kuwajima et al.,1989). We suggest that the intermediate is a premolten globule state characterized by a reduced Ca^{2+}-binding to α-LA, native -like tertiary structure, and reduced asymmetric structural fluctuation in the nanosecond time scale. The present study demonstrates the power of the method of circularly polarized luminescence for the investigation of folding/unfolding transitions in proteins.

Su-PM-C5

STUDIES OF ASSOCIATION/FOLDING PROCESSES OF THIOREDOXIN FRAGMENTS. ((María Luisa Tasayco*, Roxana Georgescu, Jian-Hua Li, Marie-Christine Petit and Stephanie Xie)) Chemistry Department, The City College of the CUNY, New York, NY 10031. (Spon. by M. Tasayco)

Profound conformational changes are thought to be involved in the mechanism of action of soluble heterodimeric toxins. To understand these changes, we have chosen to study the association/folding process between the complementary fragments of thioredoxin (Trx) (1-73 and 74-106). The individual and combined fragments of thioredoxin have been characterized using fluorescence, circular dichroism and nuclear magnetic resonance spectroscopy. The results indicate that the individual fragments are essentially random coil, but they associate with a high affinity constant (K_d in the 100 nM scale) to form a native-like heterodimeric structure reassembling Trx with reduced stability and biological activity.

Su-PM-C6

EVIDENCE FOR INTERMEDIATE STATE(S) IN THE DENATURATION OF SINGLE TRYPTOPHAN MUTANT OF BARSTAR. ((R. Swaminathan[1],Utpal Nath[2], Jayant B. Udgaonkar[2], N. Periasamy[1] and G. Krishnamoorthy[1])) [1]Tata Institute of Fundamental Research, Bombay 400 005, India and [2]National Centre for Biological Sciences, TIFR Centre, IISc Campus, Bangalore 560 012, India.

Barstar is an 89 amino acid bacterial ribonuclease inhibitor protein having 3 tryptophan side chains. A mutant of barstar having a single tryptophan (W53) was made by site-directed mutagenesis. The denaturation process of this mutant barstar by titration with GdnHCl was monitored by several probes such as CD at 220 nm or at 290 nm, fluorescence intensity, steady-state and time-resolved fluorescence anisotropy. The transition observed through the steady-state anisotropy was markedly different from others. The anisotropy was maximum around the transition region (~2M GdnHCl) and then decreased to lower values. Picosecond time-resolved fluorescence anisotropy showed that the mutant barstar has a single correlation time of 3.8 ns in the native (N) state and 1.5 ns in the unfolded (U) state (6M GdnHCl). These imply the absence of motional freedom for W53 in the N-state (3.8 ns representing the tumbling of the entire protein) and the presence of rotational freedom in the U-state. In the intermediate concentration region (1-3M GdnHCl) the anisotropy decays show at least two correlation times, 1.5 ns and 9-20 ns. These two correlation times are ascribed to partially structured forms leading to hindered rotation of W53.

Su-PM-C7

UNUSUAL STRUCTURES FORMED BY CAG DNA Triplets ((S.V.S. Mariappan[1], X. Chen[1,2], L.A. Silks III[3], R. Ratliff[2], R.K. Moyzis[2], E.M. Bradbury[2], A.E. Garcia[1] and G. Gupta[1])) [1]Theoretical Biology and Biophysics, [2]Life Sciences Division, [3]Chemical Science and Technology, Los Alamos National Laboratory, Los Alamos, NM 87545

The expansion mutation of CAG triplets is responsible for Huntington's Disease. It is our hypothesis that unusual structures, especially self-annealed hairpins, formed by these triplets cause anomalous expansion of these triplets. The sodium ion and DNA concentration dependence on the gel-mobility assay of $(CAG)_n$ [n=5 to 11] demonstrate that CAG triplets form hairpin structures exclusively at low DNA and Na^+ concentrations. However, at NMR solution conditions, $(CAG)_{5,6}$ are predominantly in the duplex form. The presence of A.A pairing and the intrahelical nature of adenines in the duplex are demonstrated by ^{15}N-labeled $(CAG)_5$ at N6 of adenines. The complete structural characterization of the hairpin or duplex of $(CAG)_{5,6}$ by NMR is not possible because of severe resonance overlap. Hence, the overlapping structural motif, GCAGC•GCAGC, present in $(CAG)_{5,6}$ is characterized by NMR and MD simulations and is used to model the hairpin and duplex forms of $(CAG)_{5,6}$. These structures will be discussed in detail. In addition, NMR imino proton profile and single strand specific enzyme-digestion experiments indicate the formation of double-hairpin structures for higher repeat number (10 and 11).

Su-PM-C8

INTERNAL DYNAMICS OF UBIQUITIN REVEALED BY NMR RELAXATION IN RANDOMLY FRACTIONALLY 13C-ENRICHED PROTEINS. ((A. Joshua. Wand, Jeffrey L. Urbauer, Robert P. McEvoy, Zhigang Li)) Department of Chemistry, State University of New York at Buffalo, Buffalo, New York 14260.

Heteronuclear NMR relaxation can potentially provide detailed information about the dynamic behavior of internuclear vectors within macromolecules such as proteins. We have developed a simple modification of existing pulse sequences which allows for the use of randomly fractionally 13C-enriched proteins in measuring spin lattice, nuclear Overhauser effects and other relaxation parameters. This experiment offers access to relaxation parameters from methine and methyl carbon sites throughout a protein using a single, easily prepared sample. We have randomly and fractionally enriched ubiquitin by expression of the protein on a mixture of labeled and unlabeled acetates. The pulse sequences used suppress contribution of 13C-13C pairs to the observed relaxation. Spin lattice relaxation and nuclear Overhauser effects have been obtained at 11.4 T and 17.6 T. The data has been analysed in the basic framework of the "model free" approach. The obtained generalized order parameters of the alpha C-H vectors of the backbone indicate highly restricted motion which is consistent with our earlier studies of the motion of amide N-H vectors. In contrast, the obtained generalized order parameters of the methine C-H and methyl symmetry axis vectors indicate a much greater range of dynamics in the core of the protein than might have been anticipated. There is significant clustering of order and disorder within the protein. The significance of these and other results will be discussed. Supported by NIH Grants GM-35940 and DK-39806.

Su-PM-C9

ENERGETICS OF HYDROGEN BONDING IN PROTEINS: A MODEL COMPOUND STUDY. ((Susan M. Habermann and Kenneth P. Murphy)) Department of Biochemistry, University of Iowa, Iowa City, IA 52242.

Differences in the energetics of amide-amide and amide-hydroxyl hydrogen bonds in proteins have been determined from the effect of hydroxyl groups on the structure and dissolution energetics of a series of cyclic dipeptides. The dissolution energetics of cyclo(L-Ala-L-Ser), cyclo(L-Ser-L-Ser), and cyclo(Gly-L-Ser) have been studied calorimetrically over a range of temperatures and compared to the dissolution energetics of cyclic dipeptides containing aliphatic side chains. The energetic effects are interpreted in light of the crystal structures of the studied compounds. Our results indicate that the amide-amide and amide-hydroxyl hydrogen bonds both provide considerable enthalpic stability to the crystalline state of cyclic dipeptides, although the amide-hydroxyl hydrogen bond is weaker. Additionally, the apolar and hydroxyl groups make positive contributions to ΔC_p of dissolution, while the peptide bond makes a negative contribution. The energetic values obtained can be used to understand the effects of mutations on the stability of globular proteins and emphasize the favorable contribution of hydrogen bonds to the enthalpy of protein folding.

Funded by the Roy J. Carver Charitable Trust.

Su-PM-C10

VERY BIG POLYSACCHARIDE MACROCYCLES: HOW, WHAT, & WHY. ((David A. Brant, Louis W. Gascoigne, and Theresa M. McIntire)) Department of Chemistry, University of California, Irvine, California 92717-2025.

Certain high molecular weight triple helical fungal glucans (e.g., schizophyllan, scleroglucan, lentinan) are of interest because of their immunostimulatory activity. The native triple helices can be dispersed as very stiff wormlike polymers in aqueous solution, where they display a helix-to-coil transition temperature $T_m = 135\ ^\circ C$ that bespeaks a remarkable stability for the helical structure. Annealing below T_m of material previously denatured by heating results in reconstitution of some native rodlike helical structures and conversion of the remainder of the material to circular structures that appear to be cyclic versions of the triple helix. The cyclic material can represent as much as 60% of the material present under some conditions of annealing temperature and concentration. We have investigated the conversion of linear triple helices to cyclic structures using non-contact atomic force microscopy, which permits ready measurements of contour length distributions and chain thickness normal to the underlying mica substrate (T. M. McIntire, R. M. Penner, and D. A. Brant, *Macromolecules*, **1995**, *28*, 6375-6377). Interpretation of these observations has been materially assisted by developing a simple equilibrium statistical thermodynamic model for triple helix formation. Supported by NIH Grant GM33062.

Su-PM-D1

THE MAGNITUDE AND INACTIVATION KINETICS OF CURRENTS OF THE α_{1E-1} AND α_{1E-3} HUMAN CALCIUM CHANNEL SPLICE VARIANTS ARE DIFFERENTIALLY REGULATED BY THE $\alpha_{2b}\delta$ AND β_{1-3} SUBUNITS. ((M. Hans, A. Urrutia, P. Brust, C. Tran, P. Sionit, K. Stauderman, M. Harpold and E. Johnson)) SIBIA, Inc. La Jolla, CA 92037.

Previously, we described that HEK293 cells expressing the human α_{1E-1}, $\alpha_{2b}\delta$ and β_{1-3} calcium channel subunits have barium currents with two-fold faster inactivation kinetics than cells expressing human α_{1E-3}, $\alpha_{2b}\delta$ and β_{1-3} subunits while other properties were unaffected. The α_{1E-3} splice variant contains a 57nt insert between α_{1E-1} nt 2240 and 2241 in the cytoplasmic loop between domains II and III. In this study, we have further examined the role of each of the α_{1E-1}, α_{1E-3}, $\alpha_{2b}\delta$ and β_{1-3} subunits in determining the inactivation kinetics and current magnitude.

Barium currents in HEK293 cells expressing either the α_{1E-1} or α_{1E-3} subunit alone inactivate rapidly, both with similar time constants (τ) of 29.1 ± 13.3 ms (n=14) and 31.2 ± 4.2 ms (n=8), respectively. The effects of the β_{1-3} subunit on inactivation depended on the α_{1E} subunit splice variant: Ba^{2+} currents in cells coexpressing α_{1E-3} and β_{1-3} subunits had slower inactivation kinetics (τ =78.9 ± 25.3 ms,n=7) than of cells expressing α_{1E-3} alone, whereas, the inactivation kinetics of cells coexpressing α_{1E-1} and β_{1-3} subunits (τ = 37.8 ± 11.4 ms, n=6) were not different from cells expressing α_{1E-1} alone. Coexpression of α_{1E} with the $\alpha_{2b}\delta$ subunit slowed inactivation kinetics of both α_{1E} subunit splice variants, but slowing was greater with α_{1E-3} $\alpha_{2b}\delta$ (τ = 80.1 ± 12.5 ms, n=6) compared to the α_{1E-1} $\alpha_{2b}\delta$ calcium channel (τ = 52.80 ± 14.3 ms, n=8). Coexpression of the $\alpha_{2b}\delta$ and/or β_{1-3} subunits in cells expressing α_{1E-1} or α_{1E-3} subunit, also markedly enhanced the current amplitude: ~5-fold with β_{1-3}, ~4-fold with $\alpha_{2b}\delta$ and ~16-fold with $\alpha_{2b}\delta$ and β_{1-3} together. The degree of enhancement did not vary with the α_{1E} subunit splice variant. These findings demonstrate that both $\alpha_{2b}\delta$ and β_{1-3} subunits can independently modulate inactivation kinetics and current magnitude of α_{1E} subunit splice variants. The results further suggest that the additional 19 amino acids encoded in the α_{1E-3} subunit modify interaction(s) with $\alpha_{2b}\delta$ and β_{1-3} subunits, and that this produces significant changes in the biophysical characteristics of the calcium channel subtypes.

Su-PM-D2

STRUCTURE OF NEURONAL (N-TYPE) VOLTAGE DEPENDENT CALCIUM CHANNELS PROBED BY ANTI-BETA SUBUNIT ANTIBODIES.
((M.W. McEnery*, W.-L. Lee, M. Pacioanu, Y. Choi, C.M. Begg, and D. J. Suciu)) Dept. of Physiology and Biophysics, Case Western Reserve University School of Medicine, Cleveland, OH 44106-4970.

N-type voltage-dependent calcium channels have been purified from two species by different procedures yet the preparations evidence considerable similarity in their apparent subunit composition (McEnery, et al., (1991); Witcher, et al., (1993); Leveque, et al., (1994)). All preparations consist of a 210-250 kDa alpha1 subunit which can be labelled by [^{125}I]omega-conotoxin, a high affinity ligand specific for the N-type VDCC, a 140 kDa protein, and associated beta subunit(s). Beta subunit isoforms comprise a family of related proteins which are required for optimal expression and function of VDCC. Whereas the beta subunit component of the rabbit brain N-type VDCC has been conclusively identified as the beta3 isoform (Witcher, et al., 1993), we observed that two putative beta subunit isoforms copurify with the N-type VDCC purified from rat brain. Thus, we were curious to pursue the possibility that the native N-type VDCC is heterogeneous in beta subunit content. To probe for beta subunit content in membranes and in the purified preparations, we prepared anti-peptide antibodies to a sequence present in all known beta subunits (beta subunit "generic" antibody). This antibody (CW20) has been used to detect multiple beta subunit isoforms that can be discriminated by their apparent molecular weights and also tissue distribution. Furthermore, CW20 has been shown to effectively immunoprecipitate [^{125}I]CTX binding from solubilized brain membranes. The native structure of the N-type VDCC present in adult rat membranes was further examined by immunoprecipitation/purification with CW20 followed by western blot analysis. Our results suggest that CW20 is an important tool which can be used to evaluate the content of native and denatured beta subunit isoforms in heterogenous samples such as rat brain membranes as well as in purified N-type VDCC.

Su-PM-D3

ELEMENTARY EVENTS UNDERLYING VOLTAGE-DEPENDENT G-PROTEIN INHIBITION OF N-TYPE Ca CHANNELS ((P. Patil, , M. de Leon, R. Reed, S. Dubel*, T.P. Snutch*, and D.T. Yue)) Johns Hopkins University & University of British Columbia*

A key regulatory mechanism of synaptic transmission is inhibition of N-type Ca channels via G-protein coupled receptors. Membrane-delimited inhibition is characterized by slowed activation, reduced peak whole-cell current, and transient reversal of inhibition by strong depolarization. There is limited single-channel information about G-protein inhibition due to the heterogeneity of receptors and channels in neurons, although elimination of a high *Po* mode of gating without change in first latency has been reported (Delcour and Tsien, *Science*, 1993). Here we reconstitute a single pathway of G-protein inhibition through transient expression of m2AChR and the N-type channel (α_{1B},β_{1b},α_2) in HEK 293 cells, enabling detailed analysis of elementary events. With expressed m2AChR, carbachol inhibits channels in a manner relieved by a prepulse (ensemble average, A). First latency (FL) is profoundly slowed, and the FL distribution (B) decomposes into slow (inhibited) and fast (uninhibited) components. The prepulse favors the fast component without changing either time constant (B, smooth). *Poo*, the probability that a channel is open at time *t* after it first opens, is unchanged by either carbachol or the prepulse (C). This excludes *Po* mode shifts, leaving slowed first latency as the sole mechanism of inhibition. Our data suggest that: (1) G-proteins impede V-dependent transitions between deep closed states, (2) The channel gates normally after overcoming this barrier, and hence (3) G proteins likely unbind for the channel to open.

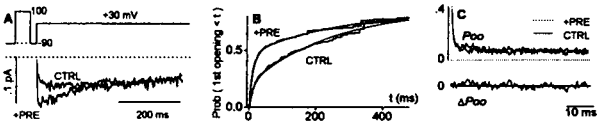

Su-PM-D4

INHIBITORY EFFECTS OF CLASSIC L-TYPE Ca CHANNEL BLOCKERS ON RECOMBINANT NEURONAL Ca CHANNELS ((D.M. Cai and D.T. Yue))
Dept. Biomed. Engr., Johns Hopkins Univ., Baltimore, MD 21205

Three classes of L-type Ca channel blockers have found widespread use as therapeutic drugs and basic research tools: dihydropyridines, phenylalkylamines, and benzothiazepines. While dihydropyridines are demonstrably selective for L-type (α_{1C}) Ca channels, the selectivity of the remaining classes is unclear because of lower α_{1C} affinity for these agents, compounded by coexistence of multiple Ca channel types in native cells. Here, we examine the effects of verapamil (phenylalkylamine) and diltiazem (benzothiazepine) upon homogeneous populations of recombinant Ca channels, including those of neuronal origin (α_{1A} & α_{1E}). Reassuringly, cardiac α_{1C}+β_2 channels expressed in mammalian HEK 293 cells reconstitute traditional inhibitory properties of native L-type Ca channels. Block is enhanced with Ca^{2+} vs. Ba^{2+} as charge carrier, lowered permeant cation concentration, and depolarization of holding potential (HP). To facilitate comparison with neuronal channels, HP = -80 mV and 2 mM Ca^{2+} is the charge carrier throughout. Half-block concentrations ($K_{1/2}$) of α_{1C}+β_2 are 110 (n=11) and 60 μM (n=14) for verapamil and diltiazem, respectively. Surprisingly, α_{1A}+β_2 and α_{1E}+β_2 are also inhibited by both agents (see below). For α_{1A}+β_2 and α_{1E}+β_2, respectively, $K_{1/2}$s are 40 (n=6) and 100 (n=9) μM for verapamil, and 270 (n=7) and 220 μM (n=11) μM for diltiazem. Our results warn against the use of verapamil and diltiazem to assess the role of L-type Ca channels in native cells, and suggest that α_{1C}, α_{1A}, and α_{1E} all possess structural elements coordinating variable interaction with phenylalkylamines and benzothiazepines.

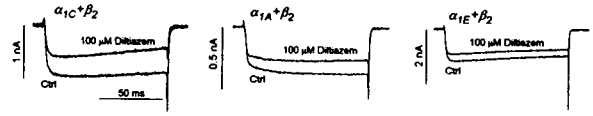

Su-PM-D5

THE ROLE OF T-TYPE CALCIUM CURRENT IN STIMULUS-SECRETION COUPLING IN AN INSULIN SECRETING CELL LINE, INS-1. ((A. Bhattacharjee, L. Wang, and M. Li)) Dept. of Pharmacology, U. of South Alabama College of Medicine, Mobile, AL 36688. (Spon. by S.D. Critz)

The functional roles of T-type voltage gated calcium channels have been difficult to ascertain, particularly in the insulin-secreting pancreatic ß-cells. We have used whole cell recordings, current clamp and capacitance measurements of the rat insulin secreting cell line, INS-1 to elucidate the importance of T-type calcium channels in stimulus-secretion coupling. By employing a double pulse protocol in the current clamp mode, we have demonstrated that the activation of T-type calcium channels depolarizes cells to an intermediary potential. As a result, the latency of onset of action potentials was decreased and the frequency of action potentials was increased. Both effects were abolished by administration of nickel, a selective T-type calcium channel blocker. Moreover, application of high frequency stimulation, as compared to low frequency stimulation, caused a greater increase in membrane capacitance (ΔCm), suggesting higher insulin secretion. We conclude that low voltage activation of T-type calcium channels enhances secretion of insulin by increasing the cell excitability. In light of the pathological implications of hyperinsulinemia, T-type calcium channels may be a therapeutic target.

Su-PM-D6

STIMULATION OF CALCIUM CHANNELS BY INTERNAL ATP IN BASILAR ARTERY SMOOTH MUSCLE CELLS (D. McHugh and D.J. Beech) Department of Pharmacology, University of Leeds, Leeds LS2 9JT, UK. (Spon. by M. Shattock)

L-type Ca channel current carried by Ca^{2+} or Na^+ is coupled to ATP metabolism in smooth muscle cells isolated from guinea-pig basilar artery. The effect did not seem to reflect an ATP- or phosphorylation requirement of Ca channel activity because in whole-cell recordings (lasting at least 10 min) Na^+ current through Ca channels ($I_{Ca(Na)}$; recorded with a divalent cation-free bath solution) was of the same amplitude with or without 9 mM ATP in the recording pipette. Furthermore, $I_{Ca(Na)}$ was maintained without ATP and when protein kinase inhibitors (H-7 and staurosporine) were in the bath and pipette, and although a subsequent 5-min exposure to the dephosphorylating agent butanedione monoxime (BDM, 50 mM) abolished $I_{Ca(Na)}$, current returned once BDM was removed. An effect of internal ATP nevertheless became apparent once the channels were blocked by internal free Mg^{2+} (0.3-2 mM). ATP inhibited Mg^{2+} block with or without a phosphorylation-supporting cocktail in the recording pipette, although AMP-PNP and AMP-PCP (which do not support phosphorylation) were ineffective. Therefore, these Ca channels did not seem to require ATP or phosphorylation for opening, but ATP relieved block by internal Mg^{2+}, perhaps via a phosphorylation-dependent mechanism. (Supported by the Wellcome Trust).

Su-PM-D7

ATP REGULATION OF Ca^{2+} CHANNELS IN ARTERIAL SMOOTH MUSCLE CELLS ((Hisashi Yokoshiki and Nicholas Sperelakis))
Dept. of Mol. & Cell. Physiology, Univ. of Cincinnati, Cincinnati, OH 45267

Inhibition of L-type Ca^{2+} channels of vascular smooth muscle cells (VSMCs) by cAMP-dependent phosphorylation, which requires Mg^{2+}ATP as a phosphate donor, has been reported (e.g., Xiong & Sperelakis, 1994), and regulation by ATP has been demonstrated (Ohya & Sperelakis, 1988, 1989) However, whether the regulation by ATP is mediated by phosphorylation has not been elucidated. In the present study, we examined effects of intracellularly perfused ATP on Ca^{2+} channel currents of isolated VSMCs from rat mesenteric arteries using a whole-cell voltage-clamp method combined with an intracellular perfusion technique. Ba^{2+} currents (I_{Ba}) through Ca^{2+} channels were evoked by depolarizing pulses (above -30 mV) from a holding potential of -80 mV with 130 mM Cs^{+} in the pipette and 100 mM Ba^{2+} in the bath. Decrease in the ATP concentration (from 5 to 0.1 mM) in the pipette caused 42 % reduction of maximal I_{Ba} obtained at +40 mV (n = 8). Increase in the ATP (from 0.1 to 5 mM) caused 61 % enhancement of maximal I_{Ba} (n = 6), and this enhancement was not prevented in the presence of 30 μM H-7, a non-specific protein kinase inhibitor. These results indicate that Ca^{2+} channels in VSMCs are regulated by intracellular ATP independent of phosphorylation, implying a direct regulatory action, such as a requirement for ATP binding to the inner surface of the channel in order for it to exhibit activity.

Su-PM-D8

G-PROTEIN ACTIVATION OF AN L-TYPE CALCIUM CHANNEL CURRENT IN HUMAN JEJUNAL CIRCULAR SMOOTH MUSCLE CELLS. ((G. Farrugia)) Mayo Foundation, Rochester, MN 55905. (Spon. by J.L. Rae)

The major calcium entry pathway in human jejunal circular smooth muscle cells is mediated through L-type calcium channels. Calcium entry is essential to sustain contractility in small intestinal smooth muscle cells. In amphotericin perforated-patch recordings, the whole cell inward current recorded with 80 mM Ba as the charge carrier is substantially less than that recorded from other regions of the gastrointestinal tract. Most of the recordings from other regions of the gastrointestinal tract have been obtained by traditional whole cell experiments with GTP in the recording pipette to prevent rundown. We examined the role of G-proteins in regulating calcium entry using traditional whole cell recordings. In cells with GTP-γS (200 μM, n=10) in the recording pipette and with 80 mM Ba in the bath as the charge carrier, the peak inward current was 188±35 pA compared with 72±4 pA (n=10) in the control group without GTP-γS ($p<0.05$). The increase in current was maximal within 60 sec of breaking into the cell. GTP-γS also appeared to shift the voltage at which peak current was observed by 15 mV. In cells preincubated with pertussis toxin (250 ng/ml, n=4) for 2 hrs, GTP-γS was without effect suggesting that the predominant G-protein(s) involved was a pertussis sensitive G-protein. The GTP-γS evoked current was blocked by nifedipine (1 μM, n=4) suggesting that GTP-γS acted on L-type calcium channels. The data suggest that pertussis sensitive G-proteins can regulate L-type calcium channels in human jejunal circular smooth muscle cells. Supported by an AGA IRSA and NIH grants DK17238, EY03282 and EY06005.

Su-PM-D9

DISTINCT SETS OF G-PROTEINS ARE RESPONSIBLE FOR INHIBITION OF CA^{2+} CHANNEL TYPES. ((Strobeck, M., Wakamori, M., Niidome, T., Nukada, T., Schwartz, A. and Y. Mori)) IMPB, Univ. of Cinti., Cinti., OH 45267-0828.

G-proteins have been shown to modify the activity of voltage-dependent Ca^{2+} channels. In particular, the neuronal ω-CgTx-GVIA-sensitive N-type and ω-Aga-IVA-sensitive P-type are reportedly susceptible to neurotransmitter inhibition via G-proteins. To molecularly clarify selective coupling of G-protein subunit subtypes with particular neuronal Ca^{2+} channel types, N (α_{1B})-, P/Q (α_{1A})-, and R(α_{1E})- type channels were expressed in baby hamster kidney (BHK) cells.

Upon intracellular dialysis of the transfected BHK cells with 0.3mM GTPγS, the N-type channel exhibited a slowing of activation and decrease in current amplitude but was recovered by administration of a positive prepulse of 80ms to +70mV. The P-type or R-type channel current, however, was not altered under the same recording conditions, although these channels were modulated by opiate receptors when coexpressed in *Xenopus* oocytes. Similar inhibition of N-type currents were induced by preincubation of the cells with cholera toxin, which constituitively activate G_s species, in the presence of GTP in the recording pipette. Northern blot analyses demonstrated that $G_{s\alpha}$ is the only abundant G_α subunit expressed in BHK cells. The expression of the other G_α's in BHK cells has been found to be very low or at undetectable levels. Thus, $G_{s\alpha}$ selectively couples with N-type channel in recombinant expression systems, suggesting difference of neuronal Ca^{2+} channel types in susceptibility to inhibitory signals evoked by neurotransmitters and hormones.

EPITHELIAL

Su-PM-E1

WATER CHANNELS AND SECRETION IN RHODNIUS MALPIGHIAN TUBULES (MT). ((C.S. Hernández, E. González, G. M. Villegas, A. Vargas-Janzen and G. Whittembury)) IVIC, IDEA, FUNDACIENCIA and UCV, POBox 21827, Caracas 1020-A, Venezuela.

MT secrete volumes (J_v) ranging from ≈0 (non stimulated, NS) to ≈100 nl/cm².s (after serotonin stimulation, SS). We explored the pathways used by J_v in MT. (I)Bath→lumen J_{21} and lumen→bath J_{12} fluxes of 19 ^{14}C or ^{3}H nonelectrolyte probes (molecular diameters, d^m ranging from water, urea, erythritol, mannitol, sucrose, to 9-30 Å dextrans) were measured together with J_v using double perfusions. (J_{21}-J_{12})= J_{net} correlated with J_v for the 8 smaller probes (d^m=3-11.8 Å) but not for the larger 11 probes. J_{net}/J_v vs d^m were linearly related (slope =-0.111 ± 0.014, $p<0.001$) for the smaller probes. These results are only fit with a single model of one monotonic function for restricted convection (not diffusion) through 11 Å-wide slits (not cylinders) which must be a paracellular water channel where the smaller solutes are dragged along. (II)Morphometric studies of NS and SS MT show that cell height decreased (from 12.4±0.8μm in NS to 8.4±0.7 in SS, $p<0.001$). Intercellular space volume density (V_v) increased (from non-detectable in NS to 7.86±0.97% in SS, $p<0.001$). We conclude that, as in other transporting epithelia (proximal tubule, gall bladder and small intestine), most of J_v is paracellular as it requires a water channel with an average width of 11 Å.
Supported by CDCH of UCV, CONICIT and Fundación Polar.

Su-PM-E2

THE ROLE OF CHOLESTEROL IN MODULATING RENAL BRUSH BORDER MEMBRANE LIPID FLUIDITY AND PHASE TRANSITIONS. ((C.J. Cruz, M.C. Giocondi, P. Wilson, C. Le Grimellec, and M. Levi.)) DVAMC, Yavneh, and Univ. of Texas Southwestern Medical Center, Dallas, Texas, and Universite Montpellier, France.

In polarized epithelial cells the apical brush border membrane (BBM) and the basolateral membrane (BLM) markedly differ from each other in lipid composition and lipid fluidity. The BBM has a significantly lower lipid fluidity as determined by the fluorescence anisotropy of DPH (r_{DPH}) and the generalized polarization of the phase-sensitive probe Laurdan ($GP_{Laurdan}$). Differential scanning calorimetry and fluorescence spectroscopy measurements as a function of temperature indicate that the BBM undergoes gel to liquid-ordered phase transition at 18°C, and liquid-ordered to liquid crystalline phase transition at 55°C. Thus at the physiological temperature of 37°C a significant percentage of the BBM lipids are in the liquid-ordered state, in fact 30% as predicted by the $GP_{Laurdan}$ measurements. Lipid fractionation studies indicate that cholesterol plays a major role in the highly ordered state of BBM lipids. In the absence of cholesterol r_{DPH} (0.210 in BBM vs 0.131 in BBM-Chol) and $GP_{Laurdan}$ (0.327 in BBM vs 0.104 in BBM-Chol) are markedly lower, which indicates a higher lipid fluidity. r_{DPH} and $GP_{Laurdan}$ measurements as a function of temperature indicate the liquid-ordered to liquid crystalline phase transition occurs at a markedly lower temperature, and $GP_{Laurdan}$ measurements estimate that at 37°C in the absence of cholesterol the BBM lipids are entirely in the liquid crystalline state. We therefore conclude that the relatively high content of cholesterol (cholesterol to phospholipid mole ratio of 0.8) plays a major role in modulating the lipid phase state and the lipid fluidity of BBM.

Su-PM-E3

PUTATIVE PHYSIOLOGICAL ROLE OF I_{sK} CHANNELS IN cAMP-MEDIATED CL^- SECRETION OF EPITHELIAL CELLS ((H. Süßbrich, M. Rizzo, S. Waldegger, F. Lang, H.-J. Lang, K. Kunzelmann, D. Ecke, M. Bleich, R. Greger and A. E. Busch)) Dept. of Physiology, Universities of Tübingen and Freiburg

The protein inducing I_{sK} channels has been found in a great variety of epithelial cells, but its physiological role in these cells remains unclear. Recently, a cAMP-regulated K^+ conductance was shown to be required for cAMP mediated Cl^- secretion of colonic crypts, and blockade of this conductance by certain cromanols was sufficient to abolish Cl^- secretion. Because I_{sK} channels are also regulated by cAMP, they may underly this conductance. We therefore tested I_{sK} channels expressed in *Xenopus* oocytes for their sensitivity to a series of cromanols and analyzed single rat colonic crypts for the expression of I_{sK} channel encoding RNA. 293B, the most potent cromanol derivative in the study of Lohrmann et al. (Pflügers Archiv, 1995), specifically inhibited I_{sK} channels with an IC_{50} of 7 μM without affecting the delayed rectifier Kv1.1 or the inward rectifier IRK1. 293B-mediated I_{sK} inhibition was not voltage-dependent and not influenced by alteration of extracellular pH. However, 293B reduced the time constant for activation (τ_{act}) at -10 mV from 13 s to 5.5 s. 434B and 407B, enantiomers of 293B, inhibited IsK with distinct IC_{50}s of 5 μM and 30 μM, corresponding to their differential potency as K^+ channel inhibitors in colonic crypts. Moreover, several other cromanols displayed the same rank order of potency for I_{sK} inhibition as was demonstrated in colon crypts. Finally, the presence of I_{sK} encoding RNA in single colon crypts was shown using the reverse transcriptase polymerase chain reaction. In summary, our data show that I_{sK} channels are the target for a novel class of K^+ channel inhibitors and indicate an important role of I_{sK} channels in colon Cl^- secretion.

Su-PM-E4

POLARIZED EXPRESSION OF K^+ CHANNELS IN *XENOPUS* OOCYTES: UNDERLYING MECHANISMS ((A. E. Busch, T. Herzer, S. Waldegger, M. P. Kavanaugh, J. P. Ruppersberg and F. Lang)) Dept. of Physiology, University of Tübingen, D-72076 Tübingen

Polarized expression of membrane proteins plays an important role in normal cell function. Little is known regarding mechanisms involved in the polarization of ion channels. In the present study we investigated the polarization of distinct K^+ channels in the commonly used expression system of *Xenopus* oocytes and the underlying mechanisms. We performed voltage-clamp experiments in the cut-open oocyte configuration and recorded current characteristics in the two oocyte hemispheres. The investigated channels were the slowly-activating I_{sK} channel, the inward rectifier IRK1 and the delayed rectifier Kv1.1. The three channels display distinct polarized expression in the animal (dark) and vegetative (light) hemisphere of *Xenopus* oocytes. I_{sK} channels are expressed in a 3:1 (dark:light) relationship, while IRK1 and Kv1.1 are expressed in a 1:9 and 1:6 (dark:light) relationship, respectively. Polarization of IRK1 and Kv1.1 was prevented when the oocytes were incubated in cytochalasin D or colchicine after cRNA injection. In contrast, cytochalasin D did not prevent polarization of I_{sK} channels, while colchicine abolished I_{sK} polarization. This suggests distinct mechanisms of trafficking for IRK1, Kv1.1 and IsK channels to their destination. Polarization of I_{sK} also affected the general properties of I_{sK}, such as the voltage needed for half-maximal I_{sK} activation ($V_{0.5}$) and its rate of activation. Finally, we tested deletion mutants of I_{sK} channels for their expression patterns. Deletions in the intracellular domain did not alter I_{sK} polarization, while specific deletions in the extracellular domain resulted in non-polarized expression of I_{sK} channels. In summary, distinct K^+ channels display specific expression patterns in *Xenopus* oocytes, which can be used to study the molecular basis of ion channel sorting.

Su-PM-E5

APICAL I_{sK} CHANNEL CURRENT IS STIMULATED BY cAMP AND INHIBITED BY PROTEIN KINASE C IN INNER EAR K^+-SECRETORY EPITHELIAL CELLS OF GERBIL. ((D.C. Marcus and H. Sunose)) Biophysics Laboratory, Boys Town National Research Hospital, Omaha, NE 68131.

It has been shown that the slowly-activating K^+ channel (I_{sK} channel) is the apical pathway for K^+ secretion in both strial marginal cells (SMC) and vestibular dark cells (VDC). In the *Xenopus* oocyte expression system, cAMP has been reported to increase I_{sK} current. Consistent with these findings, we have found in both VDC and SMC that elevation of cytosolic cAMP with the membrane permeable analog of cAMP, dibutyryl cyclic AMP or IBMX (each 1 mM) increased short circuit current and I_{sK} channel current recorded in the cell-attached, macro-patch clamp and in the nystatin-perforated whole-cell configurations. Whole-cell experiments were conducted in the absence of Cl^- to reduce the unusually high basolateral Cl^- conductance.

It has been demonstrated in the *Xenopus* oocyte expression system that stimulation of protein kinase C (PKC) inactivates the I_{sK} channel from mouse but activates the channel from guinea pig. It was therefore of interest to determine the role of PKC on the I_{sK} channel in the native epithelium of the inner ear from gerbil, the species employed in our electrophysiologic characterizations of this channel. PKC was stimulated by phorbol 12-myristate 13-acetate (PMA; 20 nM for 3 min). PMA decreased I_{sK}, g_{IsK} and V_r in both VDC and SMC . The time constant of inactivation was not changed. The inactive form of PMA, 4-α-PMA caused no significant change in any parameters for both VDC and SMC.

The present results demonstrate that the cAMP pathway up-regulates and the PKC pathway down-regulates the I_{sK} channel in VDC and SMC of the gerbil.

(This work was supported by NIH grant R01-DC00212 to DCM.)

Su-PM-E6

PROTEIN KINASE C AND A REGULATION OF A CLONED EPITHELIAL Na^+-CHANNEL. ((M.S. Awayda, I.I. Ismailov, B.K. Berdiev, C.M. Fuller, and D. J. Benos)) Dept. of Physiology and Biophysics, University of Alabama at Birmingham, Birmingham AL 35294 (Spon. by J. Bubien).

We examined protein kinase regulation of a cloned epithelial Na^+ channel (αβγ rENaC) in *Xenopus* oocytes and in planar lipid bilayers. At a holding potential of -100 mV, αβγ rENaC currents expressed in *Xenopus* oocytes averaged -1279 ± 111 nA (n = 7). A one hour treatment with 100 nM of the PKC activator, phorbol-12-myristate-13-acetate (PMA), decreased ENaC current to 17.1 ± 1.8 and 22.1 ± 2.6% (n = 7) of control, at holding voltages of -100 and +40 mV, respectively. The inactive phorbol ester, phorbol-12-myristate-13-acetate, 4-O-methyl did not alter ENaC currents. In planar lipid bilayers, addition of the catalytic subunit of PKC (5ng/ml), diacylglycerol (5μM), and Mg-ATP (100μM) decreased αβγ rENaC open probability from 0.44 ± 0.13 to 0.13 ± 0.03 (n = 9). Similar results were observed whether ENaC was obtained from an *in vitro* translation source or from oocyte plasma membrane vesicles. In contrast, ENaC studied in oocytes or planar lipid bilayers was insensitive to cAMP or direct PKA stimulation, respectively. Therefore, ENaC's, like other native epithelial Na^+channels, are inhibited by PKC but, unlike the classical vasopressin-activated Na^+-channel, are insensitive to PKA stimulation. We conclude that other associated proteins must confer PKA sensitivity to ENaC's. (Supported by NIH DK37206, NRSA DK09235, and CFF R464).

Su-PM-E7

EVIDENCE FOR AN OCCUPANCY OF SIX FOR THE WATER CHANNEL OF BOVINE CORNEAL ENDOTHELIUM. ((P. Iserovich, K. Kuang, and J. Fischbarg)). Depts. of Ophthalmol., and Physiol. & Cell. Biophysics, Coll. of P. & S., Columbia University, New York, NY 10032.

We injected 50 ng poly-A RNA from cultured bovine corneal endothelial cells into *Xenopus laevis* oocytes. We used deuterium (D_2O) to determine oocyte diffusional water permeability (P_d). Replacement of the isotonic H_2O extracellular medium by D_2O hypotonic medium produced a biphasic response: first oocytes shrank as the extracellular D_2O diffused into the cells more slowly than water exited, and then oocytes swelled in a normal osmotic response. We monitored oocyte volume changes by video microscopy. The time course of the oocyte volume fit an equation including an exponential term for the initial diffusion exchange of D_2O for water, and a nearly linear term representing the osmotic flow that followed. We calculated values for Pd from the exponential slope, and for the osmotic permeability P_f from the linear slope. The ratio P_f/P_d was 1± 0.2 in water-injected oocytes, and 5.7±1.0 (n=8) in mRNA-injected oocytes, corresponding to a single file occupancy of 5-7 water molecules per channel. If the single-file region is roughly cylindrical, from our data its length is 15-21 Å. This notion is inconsistent with the single-file region being a short constriction, but fits with recent electron crystallographic evidence for CHIP28 suggesting a narrow channel delimited at least in part by transmembrane α-helices.

Su-PM-F1

THE CONNEXIN33 PROMOTER DIRECTS THE EXPRESSION OF A LUCIFERASE REPORTER TO MALE GERM CELLS. ((L. Song, M. Chang, R. Werner and G. Dahl)) Departments of Physiology and Biophysics and of Biochemistry and Mol. Biol., University of Miami, School of Medicine, Miami, FL 33101

Connexin33 is unique among the members of the family of gap junction proteins in terms of tissue distribution and function. Based on Northern blot analysis connexin33 so far has only been found in testis. In contrast to the other connexins it does not form patent channels when assayed in paired oocytes, but specifically inhibits another connexin expressed in testis, connexin 37, to form channels. Based on these observations we have proposed the hypothesis that the function of connexin33 is to prevent homologous junctions between germ cells while allowing heterologous junctions between germ cells and Sertoli cells (Chang et. al. Biophys. J. 66, A260, 1994).

To study the expression pattern of connexin33 in more detail transgenic mice were produced harboring reporter constructs for connexin33. In a 6kb genomic rat DNA fragment containing part of the connexin33 coding region, a 3kb intron separating the 5' untranslated sequence, and 2.2kb of upstream sequence, the connexin33 coding region was replaced by the gene encoding luciferase to yield the reporter construct. Transgenic mice containing this construct express luciferase exclusively in testis at high levels (>100 x background).Thus the reporter construct exhibits the same expression pattern as connexin33. Immunohistochemical analysis of the cellular distribution of luciferase in the transgenic mice with anti-luciferase antibodies identified germ cells as the site of luciferase expression. These data support the postulated hypothesis for connexin33 function.

Su-PM-F2

MAPPING OF THE PORE OF GAP JUNCTION CHANNELS BY CYSTEINE SCANNING MUTAGENESIS. ((A. Pfahnl, X.-W. Zhou, J. Tian, R. Werner and G. Dahl)) Departments of Physiology and Biophysics and of Biochemistry and Mol. Biol., University of Miami, School of Medicine, Miami, FL 33101

The pore of gap junction channels is not accessible from the extracellular space. Similarly, the channel precursors, presumably present in the membrane in the form of hemichannels, do not allow access to the pore because the hemichannels are closed. This rule applies for most gap junction proteins (connexins) with the exception of lens connexins expressed in Xenopus oocytes (e.g. connexin46, Paul et al. J. Cell Biol. 115,1077,1991) and a chimeric connexin ($cx32E_1 43$) where in connexin32 the extracellular loop E_1 was exchanged with the corresponding sequence of connexin43.

We exploited the property of $cx32E_1 43$ and cx46 to form open hemichannels in oocytes and used the cysteine scanning mutagenesis approach (Akabas et al. Science, 258, 307, 1992) to probe for pore forming residues. Cysteines were introduced in a series of positions in transmembrane segments of both connexins. Channel inhibition by membrane impermeant maleimides applied from outside should identify residues with side chains in the pore. Strong inhibition by maleimides (which was also dependent on the size of the maleimide used) was seen in equivalent positions in both connexins: I33 and M34 in $cx32E_1 43$, and I34 and L35 in cx46. These data suggest that the M1 region of connexins contributes to the pore, possibly together with portions of M3 and the P segment.

Su-PM-F3

ANTIBODIES TO CONNEXINS BLOCK INTERCELLULAR Ca^{2+} SIGNALLING THROUGH GAP JUNCTIONS. ((Scott Boitano, *W. Howard Evans, and Ellen R. Dirksen)) Departments of Neurobiology, UCLA School of Medicine, Los Angeles, California 90095-1763 and *Medical Biochemistry, University of Wales College of Medicine, Heath Park, Cardiff, U.K. CF4 4XN.

Intercellular communication of Ca^{2+} changes occur in a variety of whole tissues and tissue culture preparations. Intercellular Ca^{2+} waves can occur spontaneously, can be initiated by application of external agonists, or can be induced by mechanical perturbation of a single cell. In the case of mechanically-stimulated intercellular Ca^{2+} waves, stimulation leads to a cell to cell communication of Ca^{2+} release from IP_3-sensitive stores. Evidence from a glial cell line suggests a requirement for gap junctions in this type of communication (Charles, et al. J. Cell Biol., **118**: 195, 1992). In the present experiments we use pulsed high frequency electroporation and digital imaging microscopy with the Ca^{2+}-sensitive dye fura-2 to evaluate the effect of sequence-specific connexin (gap junction) antibodies on intercellular Ca^{2+} waves. Electroporation of an antibody to the intracellular loop of connexin32 (Des 5, generated to amino acids 108 - 119) inhibits mechanically-induced Ca^{2+} waves in cultures of airway epithelium. Conversely, electroporation of an antibody to the extracellular loop of connexin32 (Gap 11, generated to amino acids 151 - 187) does not inhibit mechanically-induced intercellular Ca^{2+} waves in airway cell cultures. This evidence supports the hypothesis that mechanically-induced Ca^{2+} waves are propagated via gap junctional mediated events that rely on connexin 32 in the airway epithelium.

S.B. is a Parker B. Francis Fellow. This research is supported by the Tobacco Related Disease Research Program of the University of California, NASA Microgravity Research (S.B. and E.R.D.), and the Medical Research Council (W.H.E.).

Su-PM-F4

MONOVALENT ION PERMEABILITIES OF CONNEXIN PORES AND FUNCTIONAL DIVERSITY. ((R.D. Veenstra, D. A. Beblo, and H.-Z. Wang)) Dept. of Pharmacology, SUNY Health Science Center-Syracuse, NY 13210.

Single channel conductance measurements and monovalent ion selectivity sequence determinations using Cs^+, Rb^+, K^+, Na^+, Li^+, TMA^+, TEA^+, TBA^+, Cl^-, Br^-, NO_3^-, F^-, acetate$^-$, aspartate$^-$, and glutamate$^-$ have allowed us to calculate specific ion permeability values for the rat Cx43 and Cx40 channels. Equimolar ion substitutions also provide reasonable approximations of the relative cation/anion permeability of the various connexin channels we have examined to date. We have revised earlier reports of relative cation/anion selectivities based on aqueous mobilities alone to include estimates of the relative ionic mobilites within the connexin pore as a function of ionic/pore radii. These modified channel conductance-mobility plots provide more detailed predictions about the effects of charge and diameter on the permeability properties of various permeant molecules. Both rat Cx43 and Cx40 channels exhibit an Eisenman series 1 cation selectivity sequence. However, the permeability of the tetraalkylammonium ions in the Cx40 channel is significantly reduced relative to the Cx43 channel, suggesting different pore diameters and/or charge interactions for the two connexin channels. Cx40 channel conductance was only slightly affected by varying the monovalent anion in the presence of 120 mM K^+, consistent with the hypothesis that the Cx40 channel has a low anionic permeability. Molecular permeability limits are being assigned to the various connexin pores based on these ionic permeability data with obvious functional implications to second messenger signalling. Presently, species variants of Cx43 and Cx40 are being examined using this approach to narrow the search for amino acid sequence variations relevant to the observed differences in channel conductance and permeability properties of the various connexin pores.

Su-PM-F5

REGULATION OF GAP JUNCTION CHANNELS BETWEEN CELLS OF THE CIRCULAR MUSCLE LAYER IN PREGNANT RAT MYOMETRIUM ((H. Miyoshi, M.B. Boyle, L.B. MacKay, and R.E. Garfield)) Reproductive Sciences, Department of Obstetrics and Gynecology, University of Texas Medical Branch, Galveston TX 77555.

Gap junction channels are required for the propagation of electrical excitation in the contracting uterus. The relative absence of junctions helps to maintain uterine quiescence during pregnancy while their upregulation near term promotes the activity of labor. In this study, the double-whole-cell voltage-clamp method was applied to circular cell pairs freshly isolated from pregnant rat myometrium. The properties of gap junction currents in these preparations contrast in some respects to those of connexin 43 in heart and other smooth muscles. The steady-state conductance-voltage relationship is well fitted by the Boltzmann equation, yielding a voltage-insensitive fraction (g_{min}) of 0.29 ± 0.02 and half-inactivation voltages (V_h) of 58 ± 3 and -49 ± 3 mV. These parameters were smaller than expected when compared with published values for other tissues, indicating that these channels are more voltage-dependent. Unitary junctional conductance is measured as 85 pS and 25 pS under halothane exposure. These properties did not change during pregnancy. The magnitude of the junctional conductance did, however, change: 5 ± 8 nS in preterm (day 16-19) pairs, 31 ± 17 nS (day 22 term but nondelivering), and 36 ± 13 nS (day 22 delivering), and 7 ± 10 nS one-day postpartum. Thus, the conductance at delivery is at least seven-fold greater than preterm and decreases rapidly postpartum. To induce preterm labor, the antiprogesterone RU486 was injected on day 18. On day 19, when premature delivery had begun, the junctional conductance was 26 ± 17 nS vs 4.6 ± 7.9 nS (normal day 19) for controls, indicating the importance of increased electrical coupling in preterm as well as term labor. The effect of cyclic AMP, an agent which appears to rapidly reduce coupling in myometrium, was studied in cell pairs at D22 non delivering. Junctional conductance was modestly decreased by 22% with isoproterenol (10 μM) and 19% with dibutylic c-AMP (1 mM). We conclude that 1) the presence of additional gap junctions at term leads to a large increase in functional coupling between myometrial cells, 2) the channels are more voltage-dependent than in other tissues, and 3) cAMP can cause a reduction in the gap junction conductance.

Su-PM-F6

CONNEXIN 35: CLONING OF A GAP JUNCTIONAL PROTEIN EXPRESSED PREFERENTIALLY IN THE SKATE RETINA. ((John O'Brien, Muayyad R. Al-Ubaidi and Harris Ripps)) Dept. of Ophthalmology and Visual Sciences, Univ. of Illinois, Chicago, IL 60612-7242.

In the vertebrate retina, gap junctions provide pathways for the transmission of electrical signals that influence the response properties and receptive-field organization of every class of retinal neuron. We have begun to study the molecular biology of gap junction proteins (connexins) in the all-rod retina of the skate. Through low stringency screening of a skate retinal cDNA library with a rat connexin 32 clone, we have isolated clones for a novel connexin of 302 amino acids and 35 kD predicted molecular weight (Cx 35). In a northern blot analysis of mRNA from ten tissues we detected transcripts only in the retina. Hydropathy analysis and amino acid alignments reveal a long (75 aa) intracellular loop and short carboxyl terminal tail. Consensus sequences consistent with sites for phosphorylation by protein kinase C and by cAMP or cGMP-dependent protein kinase were also identified. Southern blot analysis suggests that the cloned sequence lies in a single gene with one intron. PCR amplification of this intron from genomic DNA and partial sequencing showed that it was located in the 5' end of the coding region. Multiple sequence alignments show that Cx 35 has similarities to both α and β groups of connexins and suggests that its origins may be near the divergence point for the two groups. Supported by NEI, NIAMS, and the Foundation Fighting Blindness.

Su-PM-F7

THREE-DIMENSIONAL STRUCTURE OF THE GAP JUNCTION HEMICHANNEL. ((G.A. Perkins[1], S.Ghoshroy[2], D.A. Goodenough[3] and G.E. Sosinsky[1])) [1]UCSD, La Jolla, CA 92093-0322; [2]SUNY, Stony Brook, NY 11794-5215; [3]Harvard Medical School, Boston, MA 02115.

Intercellular communication is mediated through gap junction structures that are specialized cell-cell contacts. Each gap junction contains tens to thousands of membrane channels. Each membrane channel is composed of an oligomer (called a *connexon* or *hemichannel*) of the protein, connexin. Each cell contributes a connexon and the two connexons pair at their extracellular domains to form an insulated channel. We previously showed that hydrophobic interactions predominate at the contact regions. Ca^{2+} ions are important in stabilizing the membrane pair (Ghoshroy et al., (1995) J. Membr.Biol. **146**:15-28). We have obtained images of single connexon layers or split junctions that show good lattice order. We have collected several tilt series from negatively stained split junctions and computed a three-dimensional reconstruction of the hemichannel to ~20 Å resolution. From this map, we hope to obtain information about the topology of the extracellular domains and determine how the two connexons dock to each other.

Su-PM-F8

CYCLIC NUCLEOTIDES, PH & SALT MODULATE CONNEXIN CHANNEL ACTIVITY IN LIPOSOMES ((C.G. Bevans and A.L. Harris)) Dept. Biophys., Johns Hopkins Univ., Baltimore MD 21218

Modulation of relative sucrose permeability by connexin (Cx) hemichannel activity in liposomes (PVs) was measured in the presence of cAMP, cGMP, 0.5 M KCl, pH 5.0, and pH 9.0 all relative to "standard conditions" of 10 mM KCl, pH 7.6. Rodent liver Cx was immunopurified for reconstitution (Rhee & Harris, *FASEB J.* 3:A602; rat Cx is overwhelmingly Cx32 and mouse a mixture of Cx26 and Cx32). Permeability was assayed using a transport-specific density shift effected by ultracentrifugation of reconstituted PVs on isoosmolar density gradients containing sucrose and urea as the primary solutes (Harris et al., *J. Membr. Biol.* 109:243). Reconstitution in the presence of the [^{3}H]-labeled purine cyclic nucleotides (cPMPs) greatly reduced the fraction of permeable PVs. The retention of radiolabel per liposome was similar for permeable and impermeable PVs, however the small number of permeable PVs increases the measurment error. The results were similar for both rat and mouse Cx. Earlier studies established relative permeabilities to various test molecules including permeant and impermeant dyes, fluorescently labeled linear oligosaccharides, metrizamide and nycodenz (Bevans et al. *Biophys J.* 68:A204; Bevans & Harris, ASCB 1995 Abstr.). The fraction of open channels in these permeation studies was constant despite differences in permeabilities, as they were in studies of compounds that uncouple gap junctions in cells (e.g., lidocaine, glycyrrhetinic acid). Taken together, the results suggest that cPMPs close, block or modulate the permeability of Cx hemichannels.

Continued studies of the effects of pH and salt concentration on rodent Cx show, in general, an increase in the fraction of open channels with increase in pH over the range 5-9. In addition, increasing salt concentration from 10 mM to 0.5 M greatly attenuates channel activity at all pH values. The possibilities for channel modulation suggested by these effects include: 1) global changes in protein structure mediated by pH or salt, 2) salt-mediated shielding of charges on the protein surfaces affecting channel function, and 3) titration of specific amino acid side-chains that are critical in defining channel permeability and selectivity. Support: NIH GM36044 & ONR N00014-90-J-1960.

DNA/RNA/NUCLEIC ACIDS

Su-PM-G1

THERMAL DENATURATION OF NATURAL DNA SAMPLES OF VARYING GC CONTENT: DSC STUDIES. ((*J. B. Chaires*)) Dept. of Biochemistry, Univiversity of Mississippi Medical Center, 2500 N. State St., Jackson, MS, 39216–4505

Differential scanning calorimetry was used to study the thermal denaturation of eight natural DNA samples whose GC content varied from 31 – 72%. Melting profiles varied dramatically in complexity. Procaryotic DNA samples showed simple, reversible melting curves, while eucaryotic DNA samples showed more complicated melting curves with multiple transitions. Model free enthalpy values were obtained for all DNA samples by integration of the melting curves. These enthalpy values provide a critical test for published estimates of the nearest neighbor dinucleotide melting enthalpy values (ΔH_{nn}). A comparison of published ΔH_{nn} values shows that the estimates from the Blake and Benight laboratories predict the melting enthalpies of these natural DNA samples more accurately than do estimates from the Breslauer laboratory. *Supported by NCI Grant CA35635.*

Su-PM-G2

RAMAN SIGNATURE OF THE *i MOTIF*: DNA QUADRUPLEXES CONTAINING INTERCALATED $(C{\cdot}C)^+$ BASE PAIRS IN AQUEOUS d(CCCT) AND $d(C_8)$. ((J.M. Benevides, C.-H. Kang and G. J. Thomas, Jr.)) School of Biological Sciences, University of Missouri-Kansas City, Kansas City, MO 64110.

The Raman signature of the DNA *i motif*, a quadruplex formed by intercalation of two hemiprotonated and parallel stranded cytosine duplexes, has been obtained from the spectrum of a d(CCCT) single crystal of known structure [Kang *et al.*, 1994, *Proc. Natl. Acad. Sci. USA, 91*, 11636]. Raman bands diagnostic of cytosine N3 protonation in the absence of secondary structure have also been identified. The results provide a definitive basis for evaluating both the extent of *i motif* formation in oligo-dC DNA sequences and the degree of cytosine N3 protonation. Application to aqueous d(CCCT) and $d(C_8)$ demonstrates *i motif* formation by both of these DNA sequences in solution. In the *i* form of aqueous d(CCCT), cytosine protonation is governed by pK_a (10°C) = 4.4 ± 0.2, whereas in $d(C_8)$ protonation is shifted significantly toward the physiological range, with pK_a = 5.8 ± 0.2. The present findings extend the library of Raman conformation markers to include the unusual backbone geometry and C3'-*endo/anti* conformers of deoxycytidylate residues in the novel *i* quadruplex. The significance of these results for probing solution structures of telomeric DNA sequences will be discussed. [Supported by NIH grant GM54378.]

Su-PM-G3

STRUCTURAL PREDICTION OF B-DNA DUPLEXES BASED ON COORDINATES OF THE PHOSPHORUS ATOMS. ((C.-S. Tung[1] and D.M. Soumpasis[2])) [1]Theoretical Biology and Biophysics, LANL, Los Alamos, NM 87545, [2]Biocomputation Group, Max Planck Institute for Biophysical Chemistry P.O. Box 2841, 3400 Goetingen, FRG. (Spon. by C.-S. Tung)

The Sequence-dependent structure of DNA double helices was studied extensively during the past ten years. How the backbone structure correlating to the base structure in a duplex conformation is still an important yet open question. Using a set of reduced coordinates and a least-square fitting procedure, we have developed a method to predict structures for B-DNA duplexes based on coordinates of the phosphorus atoms. This method can be used to predict all-atom structures for both bent and straight molecules. The accuracies of the predictions were estimated by studying a set of ten oligonucleotides with their structures available from PDB. We use this method to construct a modeled structure for bacteriophage λ cro-operator for which the phosphorus coordinates were known from a 3.5 Å resolution crystal data (4CRO).

Su-PM-G4

EXCIMER FORMATION IN DNA AS A PROBE OF ITS DYNAMICS AND STABILITY. ((Steven M. Kubala and Solon Georghiou)) Molecular Biophysics Laboratory, Physics Department, University of Tennessee, Knoxville, TN 37996.

Excimers (excited-state molecular complexes) in DNA are of interest because they are thought to be involved in the formation of photoproducts. We have investigated the effect of the mobility of the DNA bases on the conformation of the excimer they form by varying the solvent viscosity through the addition of sucrose to a 0.05 M sodium cacodylate, 0.1 M NaCl, pH 7 buffer solution. For these studies, we have used the polynucleotide poly(dA-dT)•poly(dA-dT), the fluorescence spectrum of which in buffer contains a monomer peak at about 325 nm and an excimer peak at about 415 nm. The excimer band is found to shift to 383 nm for η = 14 cP and to 367 nm for η = 59 cP. This decrease in the interaction energy by ~ 3000 cm^{-1} suggests that at high viscosities the mobility of the bases is greatly reduced, which results in an excimer conformation in which the overlap between the planes of the bases is considerably diminished. We have also carried out a study of the effects of methanol and acetonitrile on excimer formation. Although both of these solvents have very similar dielectric constants, the amount needed to induce DNA denaturation is found to be much smaller for the latter solvent. This suggests that specific interactions may be of importance in this process. For both solvents, the excimer-to-monomer fluorescence intensity ratio is found to undergo a large decrease for solvent amounts for which no hyperchromic changes are observed in the absorption spectrum. Thus, subtle changes in the stability of the helix strongly influence the formation of excimers. (This work was supported in part by National Institutes of Health research grant GM38236.)

Su-PM-G5

GEOMETRY AND FLEXIBILITY OF BULGED THREE-WAY DNA JUNCTIONS. ((D. P. Millar and M. Yang)) Department of Molecular Biology, The Scripps Research Institute, La Jolla, CA 92037.

Branched three-way DNA junctions occur as intermediates in various cellular rearrangements of DNA. The overall structure of three-way DNA junctions is strongly perturbed by the presence of unpaired bases at the point of intersection between helices. Unpaired bases at the branch may also introduce a point of increased flexibility in the structure. We have used time-resolved fluorescence resonance energy transfer to assess the impact of bulged bases on the static and dynamic structure of a three-way DNA junction. Donor (D) and acceptor (A) dyes were attached to the arms of a synthetic three-way junction in all pairwise combinations. Donor decay profiles were analyzed using a gaussian distance distribution model. The recovered D-A distance distributions reveal the average distance between each pair of helices, as well as the range of distances that exists between each pair. In a perfectly base-paired junction, the three inter-helix distances are approximately equal, indicating that the perfect junction adopts an extended structure. The addition of two additional non-complementary nucleotides in one of the junction strands, at the point of connection between two helices, results in a significant displacement of one of the helices, while the position of the other helix remains relatively fixed. Moreover, the nature of the bulged bases dictates which of the flanking helices is perturbed by the bulge. Thymine, cytosine and adenine bulges specifically perturb the helix on the 3' side of the bulge, whereas a guanine bulge perturbs the helix on the 5' side of the bulge site. In addition, there is a broad range of distances between the perturbed arm and each of the two fixed arms in the bulged junctions, indicating that the perturbed arm has high mobility. Supported by NSF grant MCB-9317369.

Su-PM-G6

THE SEARCH FOR RIGIDITY IN DNA NANOCONSTRUCTION. ((Jing Qi, Xiaojun Li, Xiaoping Yang, and Nadrian C. Seeman)) Department of Chemistry, New York University, New York, NY 10003.

We have synthesized a cube and a truncated octahedron from DNA in the past. We wish to extend this capability to the construction of periodic matter, which entails translational symmetry. Molecular construction that involves high symmetry requires at least 3 elements: [1] Predictable specificity between components, [2] structural predictability of intermolecular products; and [3] structural rigidity of components. DNA branched junctions satisfy the first two requirements, but lack rigidity. A rigid DNA component is one in which the directions of double-helix axes (and hence the angles between them) vary within limits of flexibility no greater than those of linear DNA. We have tested the rigidity of triangles constructed from bulged 3-arm branched junctions. Triangles that alternate bulges on the inside and outside strands provide a reporter strand (thick strand below) for cyclization experiments.

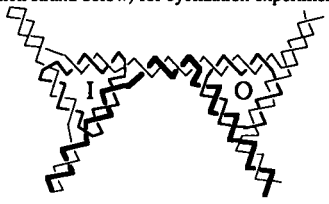

Supported by grants from ONR, NIH and W.M.Keck.

Su-PM-G7

STABILITY AND CONFORMATION OF $[d(T)-d(A)-d(T)]_n$. ((Y.Z. Chen and E.W. Prohofsky)) Purdue University, Dept. of Physics, W. Lafayette, IN 47907-1396.

A statistical mechanical variation of a vibrational mode, internal fluctuations, and hydrogen bond disruption of a DNA triplex was performed on both the fiber diffraction model with N-type sugar conformation and a proposed model with a S-type sugar conformation. Our modes for the S-type structure are in good agreement with observed IR spectra. Large discrepancies are found between observed modes for the N-type structure. The contribution of internal fluctuations to free energy, premelting hydrogen bond disruption probability and hydrogen bond melting temperatures for the Hoogsteen and Watson-Crick hydrogen bonds all show that the S-type structure is dynamically more stable than the N-type structure. Our calculation indicates $[d(T)-d(A)-d(T)]_n$ most likely adopts a S-type sugar conformation in solution.

Su-PM-G8

NON-CONTACT HANDLING OF μm-SIZED PARTICLES USING ULTRASOUND. ((K. Yasuda, +K. Takeda and S. Umemura)) Advanced Research Lab., HITACHI Ltd., 2520 Akanuma, Hatoyama, Saitama 350-03, JAPAN and +Central Research Lab., HITACHI Ltd., Kokubunji, Tokyo 185, JAPAN. (Spon. by H. Takei)

The efficacy of using an ultrasonic standing plane wave to concentrate small particles in a liquid was theoretically estimated and compared with experimental results [1]. The theory predicts that the effect of diffusion is negligible in concentrating polystyrene spheres larger than 5 μm in diameter when they are subjected to 4 J/m^3 ultrasound at 500 kHz. The halfwidth of the steady-state particle distribution in the experiment was in the same order of magnitude as in the theory. This technique was applied to concentration of biomaterials like DNA, red blood cells and liposomes. After the ultrasonic irradiation started, 3kbp DNA clusters in ethanol solution started moving toward the pressure node of the ultrasonic stationary standing wave and then gathered to form a larger cluster [2]. Liposomes also gathered to the pressure node by the acoustic radiation force. The halfwidth of the liposome distribution depended on the difference between the density of the solutions outside and inside the liposome. The separation of particles in liquid by competition between acoustic radiation force and electrostatic force was also tested. The displacement of particles from the pressure node of an ultrasonic standing wave is expected to vary according to the effective charge, radius and stiffness of the particles. By application of this technique, a mixture of polystyrene spheres with two different radii was successfully separated according to their radii.

1) Yasuda, K. et al (1995) Jpn. J. Appl. Phys. **34**, 2715-2720.

2) Yasuda, K. et al (1996) J. Acoust. Soc. Am. in press.

ACTIN AND ACTIN BINDING PROTEINS

Su-Pos1

THE STRUCTURE OF YEAST F-ACTIN. ((A. Orlova[1], P. Rubenstein[2] and E.H. Egelman[1])) [1]Dept. of Cell Biology and Neuroanatomy, Univ. of Minn. Medical School, Minneapolis, MN 55455; [2]Department of Biochemistry, Univ. of Iowa College of Medicine, Iowa City, Iowa 52242.

While there is a strong tissue-specificity to the different isoforms of actin, little structural data exists on the differences between filaments formed by these different isoforms. We have used electron microscopy and three-dimensional reconstruction to study yeast actin, as well as a mutant yeast actin. While all actins are substantially conserved across evolution, yeast and rabbit muscle actins are only 87% conserved in primary sequence. We have found that under different conditions (with either Mg^{2+} or Ca^{2+}) the yeast actin appears to display less extensive contact between the two long-pitch helical strands when compared to muscle actin. The S14A mutation in yeast actin (Chen and Rubenstein, JBC **270**, 11406-11414, 1995) involves a mutation at a residue that is assumed to bind to the γ-phosphate of ATP. It has been shown that this mutation has a 40-60 fold decrease in actin's affinity for ATP (Chen *et al.*, JBC **270**, 11415-11423, 1995). We show that this single substitution appears to modulate the cleft between the two lobes of the actin subunit. We have also found that the yeast actin displays the large-scale cooperativity that we previously observed for muscle actin (Orlova *et al.*, JMB **245**, 598-607, 1995).

Su-Pos2

MICROSECOND ROTATIONAL DYNAMICS OF F-ACTIN IN ACTO-S1 COMPLEXES DURING STEADY STATE ATP HYDROLYSIS. ((C.A. Rebello & R.D. Ludescher)) Department of Food Science, Rutgers-The State University of New Jersey, New Brunswick, NJ 08903-0231.

We have monitored the microsecond rotational dynamics of rabbit skeletal muscle F-actin, in acto-S1 complexes in rigor and during steady state ATP hydrolysis, by using the steady state phosphorescence emission polarization from a phosphorescent probe, erythrosin-5-iodoacetamide, covalently attached to cys-374 of actin. This probe is sensitive to rotational motions in F-actin on the micro- to millisecond time scale. For the 1:1 acto-S1 complex the anisotropy of the rigor complex and of the complex during steady state ATP hydrolysis were 0.135±0.004 and 0.064±0.006, respectively. The corresponding values for a 10:1 acto-S1 complex were 0.137±0.002 and 0.067±0.002 respectively. The emission anisotropies of these two complexes during active ATP hydrolysis were lower than that of the F-actin filament, 0.077±0.003, suggestive of S1 induced rotational motions in F-actin during ATP hydrolysis. Since even at sub-stoichiometric acto-S1 ratios, i.e. 10:1, the phosphorescence emission anisotropies were not significantly different from that of the 1:1 acto-S1 complex, both in rigor and during steady state ATP hydrolysis, we conclude that F-actin undergoes some degree of cooperative rotational motions during steady state ATP hydrolysis. (Research supported by the Muscular Dystrophy Association).